Spacecraft Mission Design for the Optimal Impulsive Deflection of Hazardous Near-Earth Objects (NEOs) using Nuclear Explosive Technology

Brent William Barbee[*]
Emergent Space Technologies, Inc., Greenbelt, MD, 20770

Wallace T. Fowler[†]
The University of Texas at Austin, Austin, TX, 78712

The collision of a moderately large asteroid or comet, also referred to as a Near-Earth Object (NEO) with Earth would have catastrophic consequences. To address this threat, we present a completely generalized hazardous NEO scenario timeline and associated spacecraft mission design architecture for hazardous NEO response that is intended to provide a means for designing missions to successfully deflect any arbitrary NEO predicted to have a significant likelihood of future collision with Earth. A generalized algorithm for optimizing the deflection of a NEO via a single impulse is presented and applied to the case of the asteroid Apophis, an asteroid that will closely approach Earth at an altitude of approximately 32000 km on April 13th, 2029 and may pass through a gravitational keyhole at that time, which would cause Apophis to collide with Earth in 2036. The case study performed on Apophis includes preliminary trajectory design that identifies the most favorable launch windows between 2008 and 2036 and computes how much spacecraft mass can be efficiently brought to rendezvous with the asteroid at each launch opportunity for two possible spacecraft launch vehicle and thruster combinations. The use of nuclear explosives as NEO deflection mechanisms is discussed in terms of the underlying theory, advantages, and disadvantages. The Apophis case study concludes with the presentation of optimal deflection results for the asteroid indicating by how much it can be optimally deflected at any time between the current time and shortly before the 2029 close approach. Trends in the optimal deflection data and the sensitivity of the optimal solutions are identified and discussed. An outline of a campaign of missions to Apophis for the purposes of characterization and, if necessary, deflection is presented. Paths for future research and algorithm development indicated by the current results are also discussed.

I. Introduction

THE collision of a moderately large asteroid or comet, also referred to as a Near-Earth Object (NEO) with Earth would have catastrophic consequences. Such events have occurred in the past and will occur again in the future. However, for the first time in known history, humanity may have the technology to counter this threat. NEOs of sufficient estimated mass, sufficient predicted Earth impact velocity, and for which there is significant perceived probability of future Earth impact are considered hazardous[‡].

---

[*] Aerospace Engineer, Aerospace Systems & Technology Division, AIAA Member, email:
brent.barbee@emergentspace.com
[†] Professor, Aerospace Engineering and Engineering Mechanics, The University of Texas at Austin, Paul D. and Betty Robertson Meek Centennial Professor in Engineering, Director, Texas Space Grant Consortium, University Distinguished Teaching Professor, and Fellow, AIAA, email: fowler@csr.utexas.edu
[‡] Definitions for "sufficient estimated mass and predicted Earth impact velocity" and "significant perceived probability of future Earth impact" are currently somewhat vague. For more information, the reader may investigate the Torino and Palermo scales, which are the two currently accepted scales for assigning a hazard rating to a NEO.

This paper presents a generalized hazardous NEO scenario timeline and an associated generalized hazardous NEO response mission design architecture. The timeline and architecture were both designed to be applicable to any conceivable hazardous NEO scenario. The timeline presents all the events that should occur from the beginning to the end of a hazardous NEO scenario, beginning with humanity's discovery and recognition of the threat and culminating in the attempt (which is hopefully successful) to deflect the NEO and thereby prevent the collision of the NEO with Earth.

No new space hardware technology is predicted to be available; rather, current space hardware technology is assumed. Additionally, it is assumed that the chosen means of eliminating a hazardous NEO is a single impulsive deflection of the NEO, particularly via a nuclear explosive detonated in proximity to the NEO. Nuclear explosives offer the highest energy density of any known or foreseeable technology, by several orders of magnitude, and hence are the clear choice in terms of achievable payload masses for NEO deflection spacecraft using current launch and space propulsion technology. However, nuclear explosives have never been tested in space, much less on a NEO. Thus, their effectiveness, while predicted to be sufficient, has yet to be characterized and so the basic theory behind using a nuclear explosive to impulsively deflect a NEO is presented and discussed briefly but is not elaborated upon further. Deflection of the NEO is selected as the means of eliminating the threat because it requires less energy than fragmenting and dispersing the NEO. Furthermore, complete annihilation (e.g., vaporization or pulverization into a fine-grain dust cloud) of a NEO is well beyond the capabilities of current or foreseeable technology.

An algorithm for optimizing an impulsive NEO deflection is derived and discussed, along with the general structure of the software that implements the algorithm. The algorithm is designed to treat the specific case of a single impulse applied to the NEO but is otherwise completely general and unconstrained. In particular, it does not depend on the deflection mechanism, assuming only that the deflection is impulsive in nature.

An optimal deflection case study was performed on the asteroid Apophis in the 2006 to 2029 timeframe. Numerical results are presented and discussed.

Finally, the overall results of the studies undertaken for this paper are summarized and conclusions are presented, including the structure of a recommended campaign of missions to Apophis. Future work paths in optimal NEO deflection and hazardous NEO response mission design are enumerated.

II. Spacecraft Mission Design for Hazardous NEO Response

Discussion of the appropriate response to a hazardous NEO scenario identifies the sequence of key events, provides a framework within which an effective mission design architecture for threat response can be designed, and illustrates the means by which hazardous NEO response can be optimized.

A. Hazardous NEO Scenario Timeline

The hazardous NEO scenario timeline is presented graphically in Fig. 1. The timeline begins with the initial detection of the NEO. Time is then required to ascertain whether the NEO is indeed hazardous because radar observations of the NEO from Earth must be accumulated and processed for NEO orbit determination and Earth collision prediction. The amount of time required to firmly establish that a NEO does indeed have a sufficient probability of Earth collision to warrant further action is a function of the accuracy and quantity of the orbit measurements, which is largely dictated by the observability of the NEO and relative geometry between the NEO and Earth, which determine how often observation arcs are available and their length. More frequent and longer observation arcs greatly decrease the amount of time required to make a firm NEO threat assessment.

Once it has been determined that the NEO has a sufficient probability of Earth collision to warrant action, mission planning for deflection of the NEO begins immediately. A certain amount of time must be devoted before construction of the spacecraft and launch vehicle may begin. The time of launch depends on how quickly the spacecraft and launch vehicle can be readied and the relative positions of Earth and the NEO in their orbits. Additional time will be required for the spacecraft to complete the rendezvous with the NEO and to deploy and prepare the deflection mechanism for activation. The earliest time that a deflection is possible marks the start of the interval during which the deflection may be applied. This interval ends shortly before the time at which the NEO would collide with Earth absent human intervention.

As will be demonstrated, the earlier the deflection is performed, the greater the amount by which the NEO can be pushed away from Earth. This can be achieved by expanding our ability to see and track NEOs, using Earth-based observatories and orbital observatories. Earlier deflections are also enabled by the ability to build and launch a NEO response spacecraft quickly. We can develop this capability by performing more NEO rendezvous missions for the

purposes of science and deflection system testing since this will improve our ability to design and deploy missions to NEOs quickly. Together, early NEO detection and the ability to build and launch deflection spacecraft quickly serve to minimize the time blocks in the timeline for detection, threat determination, and designing a response mission and preparing it for launch. Finally, optimizing the NEO rendezvous to minimize flight time within the constraints of spacecraft launch and propulsion technology will minimize the time required to complete NEO rendezvous. All of this maximizes the size of the continuum of available deflection times.
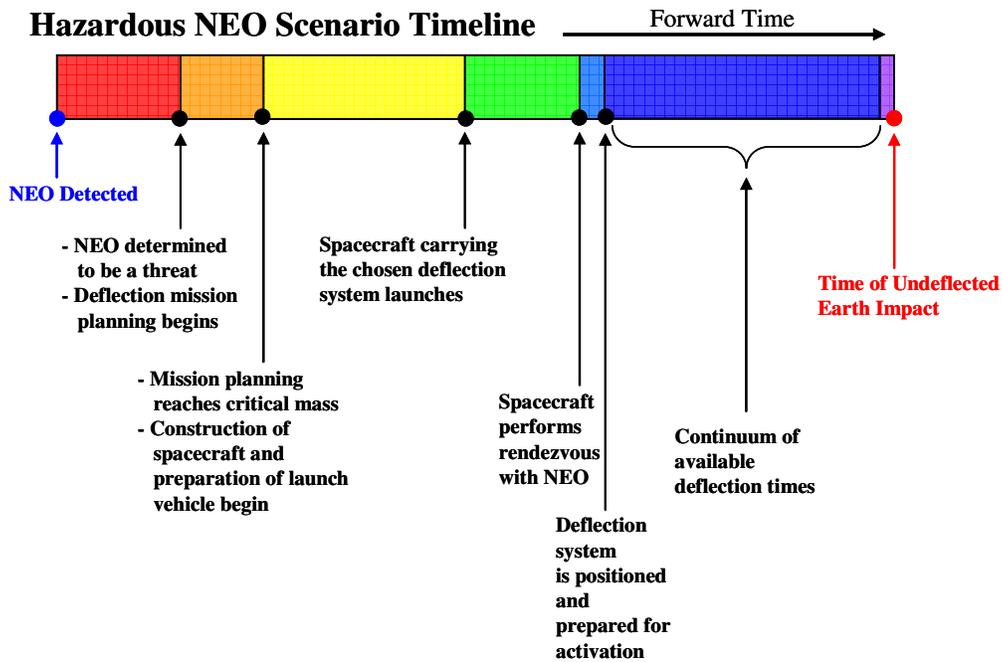
Hazardous NEO Scenario Timeline

Forward Time

NEO Detected

- NEO determined
  to be a threat
- Deflection mission
  planning begins

- Mission planning
  reaches critical mass
- Construction of
  spacecraft and
  preparation of launch
  vehicle begin

Spacecraft carrying
the chosen deflection
system launches

Spacecraft
performs
rendezvous
with NEO

Deflection
system
is positioned
and
prepared for
activation

Continuum of
available
deflection times

**Time of Undeflected
Earth Impact**

Figure 1. Hazardous NEO scenario timeline.

B. Spacecraft Mission Design Architecture

A decision process for designing missions to respond to hazardous NEOs is presented in Fig. 2. The process begins with the initial detection of the NEO and concludes with the execution of the deflection mission.
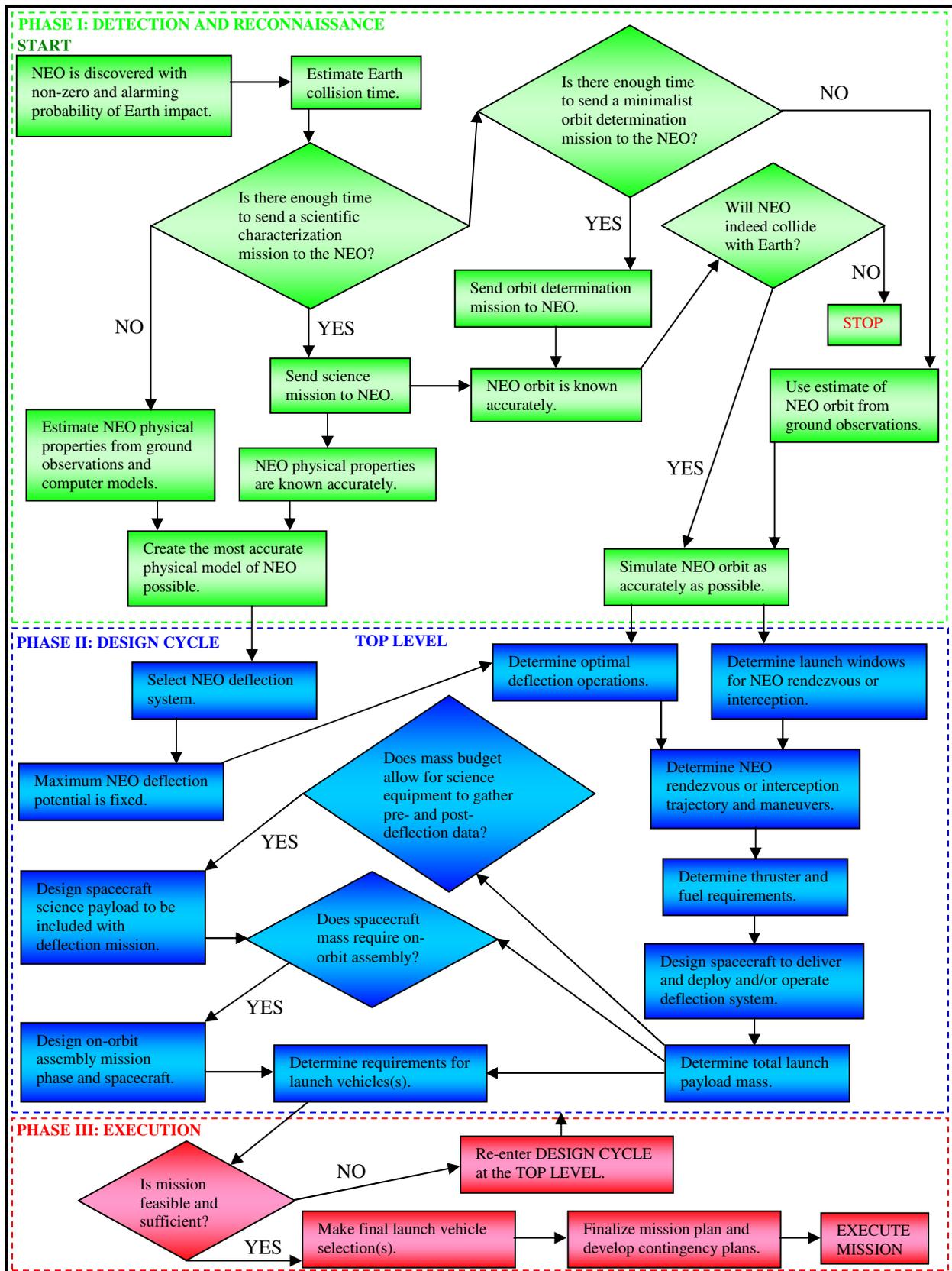
PHASE I: DETECTION AND RECONNAISSANCE
START

NEO is discovered with non-zero and alarming probability of Earth impact.

Estimate Earth collision time.

Is there enough time to send a scientific characterization mission to the NEO?

Is there enough time to send a minimalist orbit determination mission to the NEO? — NO

Will NEO indeed collide with Earth? — NO

NO

YES

Send orbit determination mission to NEO.

YES

STOP

Send science mission to NEO.

NEO orbit is known accurately.

Use estimate of NEO orbit from ground observations.

Estimate NEO physical properties from ground observations and computer models.

NEO physical properties are known accurately.

YES

Create the most accurate physical model of NEO possible.

Simulate NEO orbit as accurately as possible.

PHASE II: DESIGN CYCLE   **TOP LEVEL**

Select NEO deflection system.

Determine optimal deflection operations.

Determine launch windows for NEO rendezvous or interception.

Maximum NEO deflection potential is fixed.

Does mass budget allow for science equipment to gather pre- and post-deflection data?

Determine NEO rendezvous or interception trajectory and maneuvers.

YES

Determine thruster and fuel requirements.

Design spacecraft science payload to be included with deflection mission.

Does spacecraft mass require on-orbit assembly?

Design spacecraft to deliver and deploy and/or operate deflection system.

YES

Design on-orbit assembly mission phase and spacecraft.

Determine requirements for launch vehicles(s).

Determine total launch payload mass.

PHASE III: EXECUTION

Is mission feasible and sufficient? — NO

Re-enter DESIGN CYCLE at the TOP LEVEL.

YES

Make final launch vehicle selection(s).

Finalize mission plan and develop contingency plans.

EXECUTE MISSION

Figure 2. Hazardous NEO response decision process flowchart.

III. Optimal Impulsive NEO Deflection Theory

A method is presented for optimizing the application of a single impulsive velocity change to a NEO, for the purpose of deflecting it. For an impending close approach, it is desired to move the NEO's close approach distance as far away from Earth as possible. For an impending collision, it is desired to cause the NEO to not collide with Earth while passing by Earth at the maximum distance possible.

The relevant geometry is shown in Fig. 3 in the Heliocentric Inertial (HCI) reference frame. The distance between the NEO and the Earth is a function of time as each body orbits the Sun and is denoted by Δr.
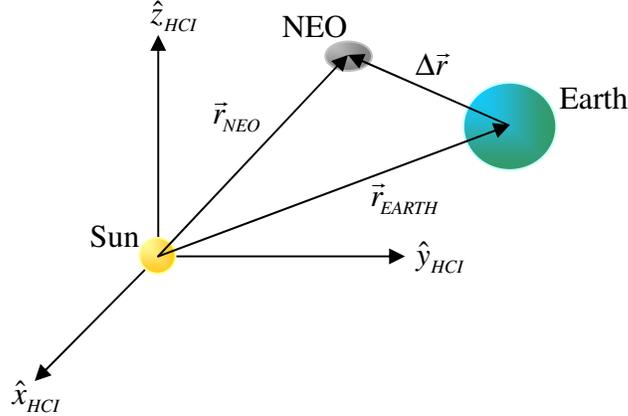
Figure 3. HCI frame NEO and Earth absolute positions and NEO-Earth relative position.

A collision occurs if the condition shown in Eq. (1) is true.

$$\Delta r(t_{COLL}) = R_{EARTH} \tag{1}$$

At the time of collision, denoted by t_{COLL}, the distance between the NEO and Earth will be equal to the Earth's equatorial radius[*], denoted by R_{EARTH}, constituting a collision[†]. For the case in which the NEO closely approaches Earth but does not collide, the distance between the NEO and Earth at the time of closest approach is denoted by $\Delta r(t_{CA})$ where t_{CA} is the time of close approach. By definition this distance is greater than R_{EARTH} by some amount since a collision does not occur.

Since we desire to deflect the NEO, we must apply an impulse to it at some time prior to the event time, whether it be t_{COLL} or t_{CA}. Let us denote the time at which the deflection is applied as t_{DEF} and the NEO's true anomaly at the time of deflection as v_{DEF}.

The application of an impulsive velocity change maneuver to the NEO for the purpose of deflection is depicted in Fig. 4. The goal of the optimization is to determine the optimal time at which to apply the deflection, t_{DEF}, and the optimal deflecting impulse, $\Delta \vec{v}$. We will first define the appropriate performance index for this problem and then specify the complete set of parameters that must be determined in order to completely specify a solution. The performance index is the distance between the Earth and the NEO at closest approach. This index, P, is presented as a function of the undeflected trajectory and its deflected counterpart in Fig 5. There will be a closest approach of Earth by the NEO on both trajectories and the ultimate goal is to cause the NEO to miss the Earth.

---

[*] The Earth's equatorial radius, 6378.137 km, is used here to define a bounding sphere about the Earth for the purposes of defining when a collision occurs geometrically.
[†] The bounding sphere around the NEO is assumed to be small enough in comparison to Earth's bounding sphere that it may be neglected and the NEO treated as a point mass for the purpose of geometric collision definition.
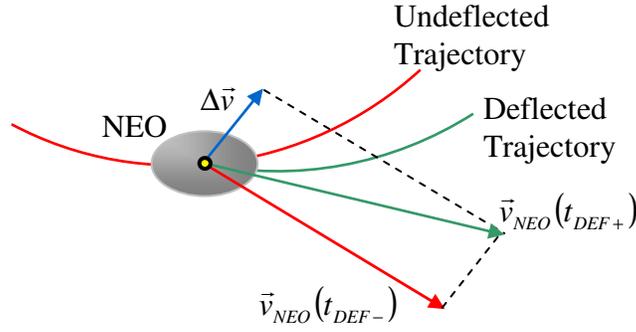
Figure 4. Application of an impulsive velocity change maneuver to a NEO for the purpose of deflection.
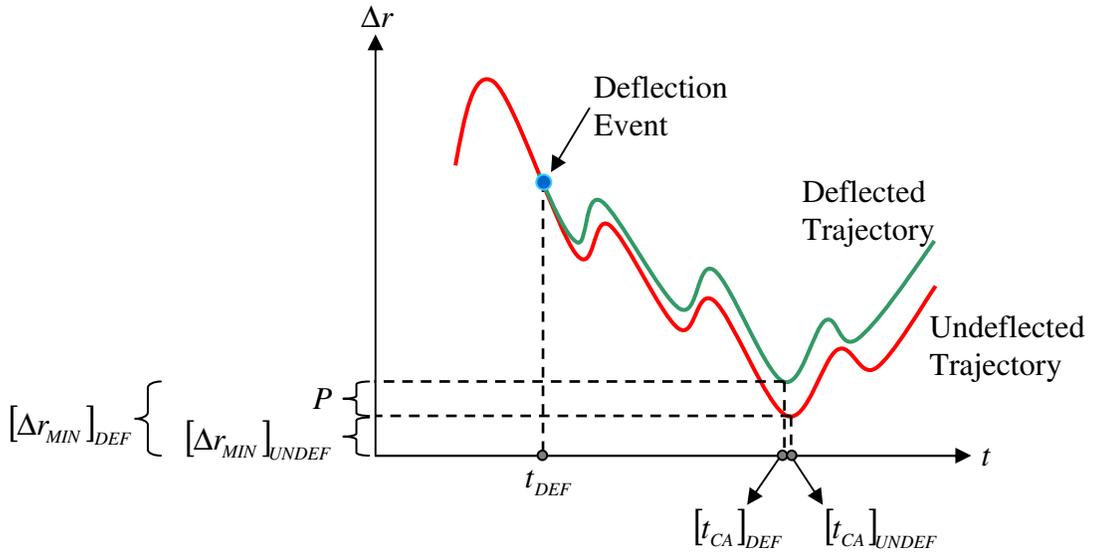

Figure 5. Graphical presentation of the performance index for optimizing a NEO deflection.

Note that the subscript *DEF* refers to the deflected NEO trajectory and the subscript *UNDEF* refers to the undeflected NEO trajectory. The minimum NEO-Earth distance on the undeflected trajectory is denoted by $\left[\Delta r_{MIN}\right]_{UNDEF}$ and the minimum NEO-Earth distance on the deflected trajectory is denoted by $\left[\Delta r_{MIN}\right]_{DEF}$. Thus the performance index is written as shown in Eq. (2), denoted by P.

$$P = \left[\Delta r_{MIN}\right]_{DEF} - \left[\Delta r_{MIN}\right]_{UNDEF} \tag{2}$$

For any given scenario, $\left[\Delta r_{MIN}\right]_{UNDEF}$ only needs to be computed once since it is a constant. However, $\left[\Delta r_{MIN}\right]_{DEF}$ is a function of the deflection parameters and must be computed every time P is evaluated during the optimization. We have already established that one parameter in the optimal solution is the time at which the deflection is applied, t_{DEF}, but it remains to specify the remaining parameters, all of which are involved in specifying the applied deflecting velocity change, $\Delta\vec{v}$.

Figure 6 shows the applied impulsive velocity change for deflection in the NEO's Radial, In-Track, Cross-Track (RIC) reference frame at the time of deflection along with the parameters that define it. The $\Delta\vec{v}$ is parameterized by its magnitude, Δv, and two spherical coordinate angles, azimuth (α) and elevation (δ). A third angle is also

introduced, called the velocity angle (θ), which lies in the plane defined by $\Delta\vec{v}$ and the NEO's velocity vector expressed in the RIC frame, denoted by $[\vec{v}_{NEO}(t_{DEF-})]_{RIC}$. Note that – and + signs in the t_{DEF} subscript distinguish between the instant in time immediately prior to deflection and the instant in time immediately after. This concept was expressed graphically in Fig. 4.
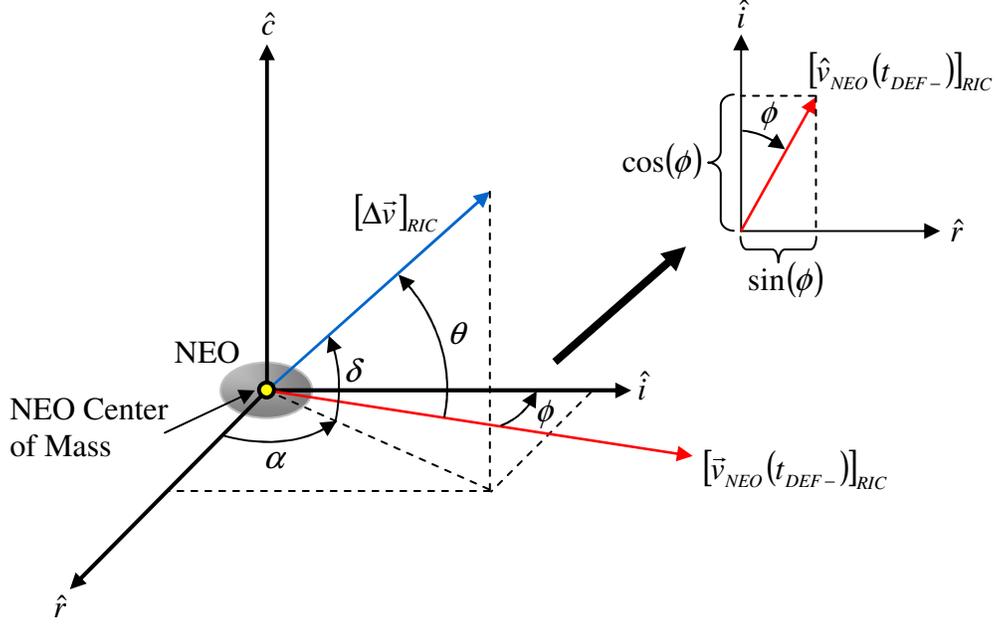

Figure 6. Applied deflecting impulse vector geometry in the NEO's RIC frame at the time of deflection.

Following the conventions shown in Figs. 4 and 6, the application of the deflecting impulse vector is expressed mathematically as shown in Eq. (3). Note that the matrix $T_{HCI}^{RIC}(t_{DEF-})$ in Eq. (3) is the time-dependent transformation matrix that transforms vectors from the RIC frame to the HCI frame and is always constructed at the instant in time immediately prior to the deflection.

$$[\vec{v}_{NEO}(t_{DEF+})]_{HCI} = [\vec{v}_{NEO}(t_{DEF-})]_{HCI} + T_{HCI}^{RIC}(t_{DEF-})[\Delta\vec{v}_{RIC}] \tag{3}$$

Figure 6 also shows the applied deflecting impulse vector in terms of the spherical coordinate angles and its magnitude, as shown in Eq. (4).

$$\Delta\vec{v}_{RIC} = \Delta v \begin{bmatrix} \cos(\alpha)\cos(\delta) \\ \sin(\alpha)\cos(\delta) \\ \sin(\delta) \end{bmatrix} \tag{4}$$

Thus the applied impulse vector is expressed in terms of three intuitive quantities. Fig. 6 also presents an angle, ϕ, which is the flight path angle of the NEO. This angle is used to facilitate the relationship between the velocity angle, θ, and the two spherical coordinate angles, α and δ, given in Eqs. (5) and (6). Note that the range of the velocity angle is $0 \le \theta \le \pi$.

$$\theta = \arccos([\Delta\hat{v}]_{RIC} \cdot [\hat{v}_{NEO}(t_{DEF})]_{RIC}) \tag{5}$$

$$\theta = \arccos(\sin(\phi)\cos(\alpha)\cos(\delta) + \cos(\phi)\sin(\alpha)\cos(\delta)) \tag{6}$$

The velocity angle is used to characterize the angle between the optimal deflecting impulse vector and the NEO's velocity vector. Figure 7a shows the variation of the flight path angle through its entire range of motion for the asteroid Apophis, the asteroid which is the subject of a case study in a subsequent section. Fig. 7a indicates that ϕ varies between approximately $\pm 11°$. Figure 7b shows all possible values of θ in azimuth-elevation space for a nominal value of ϕ, according to Eq. (6). The entire range of possible ϕ values was considered but the results were found to not vary appreciably so only one surface plot is shown.

(a)	(b)
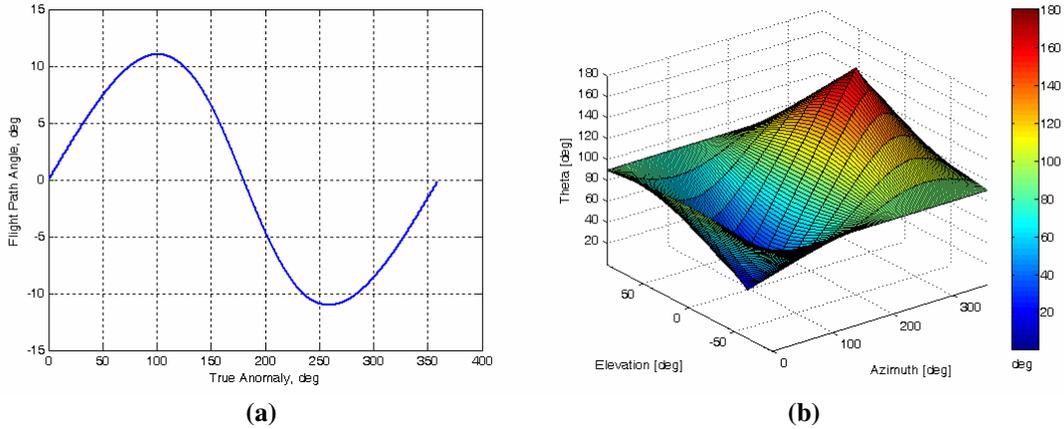
Figure 7. (a) Variation of the flight path angle throughout one orbit for Apophis and (b) variation of velocity angle through all values in azimuth-elevation space for a nominal flight path angle value.

While an optimal velocity angle, θ, will be computed in the post-processing of deflection data in order to characterize the orientation of a deflecting impulse vector with respect to the NEOs' velocity vector direction, θ itself is not one of the parameters that is directly solved for as part of the optimization process.

Thus the parameters that completely specify a NEO deflection are t_{DEF}, Δv, α, and δ. The goal of the optimization is to find the combination of these four quantities that maximizes the deflection, according to the performance index in Eq. (2). The ranges of possible values for each quantity form the parameter space for the deflection problem, which in turn maps to a space of performance index values, as shown in Fig. 8 for clarity.
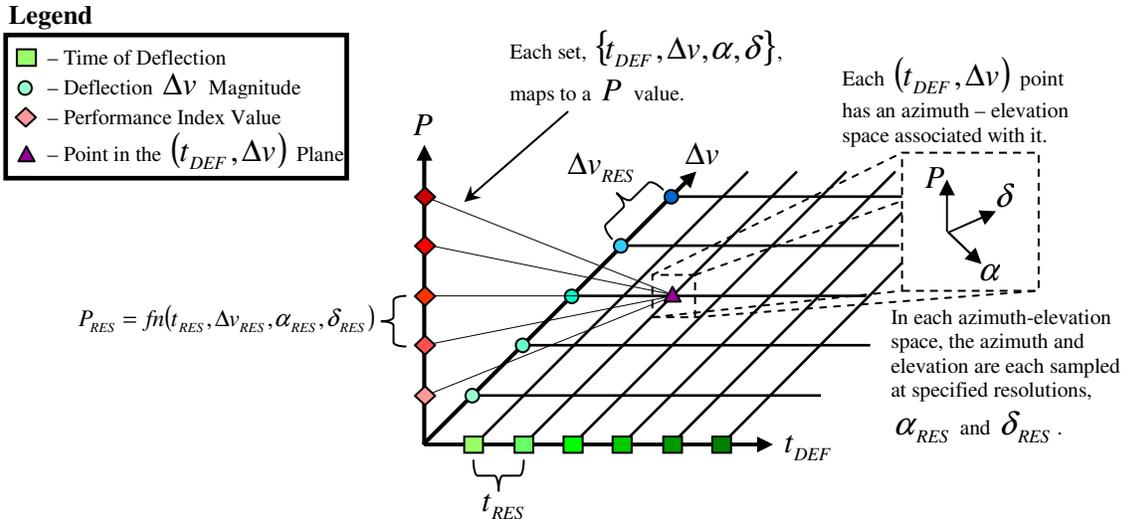

Figure 8. Complete single impulse optimal NEO deflection parameter and solution space.

Previous research has indicated that there is always a global optimum for P (Ref. 1). Figure 8 also shows that each of the four parameters are sampled at a given resolution along their respective axes. Note that the resolution

along an axis does not have to be constant, nor does the resolution at which one parameter is sampled have to be equal to any other resolution.

Thus, the single impulse optimal NEO deflection problem is a multi-dimensional non-linear optimization problem. The non-linearity arises in the mapping of a given set of deflection parameters to the corresponding performance index value. This requires the numerical integration of the NEO's heliocentric orbit including the applied impulse. In order to achieve sufficient accuracy, particularly over the long time scales (in the several tens of years, preferably) involved, the force models used in the propagation of the NEO's deflected state must be of sufficient fidelity. Previous research determined that the force model must at least include the effects of the Sun's gravity and the Earth's gravity on the NEO[1] and this is the force model utilized in this study. Future research will examine the effects of utilizing higher-fidelity force models that include the gravity of other planets, solar radiation pressure, and the Yarkovsky effect, which is anisotropic thermal re-radiation from the NEO's surface during its rotation about its spin axis. Increasing the complexity of the force model also dramatically increases the computational expense associated with evaluating the performance.

It is important to note that the large mass of any given NEO, combined with current and foreseeable technology levels, means that the best we can do is perturb the NEO's state. Thus, if the undeflected event is a collision, at best we will cause the collision event to transition to a close approach event. If the undeflected event is a close approach, at best we will cause it to transition to another close approach at a greater distance.

Determining the optimal solution requires the definition of four vectors of design space parameters: a vector of deflection times, a vector of applied impulse magnitudes, a vector of azimuth angles, and a vector of elevation angles. The performance index specified in Eq. (2) is computed for each element in the set of unique combinations of all elements in the four vectors of deflection parameters.

The performance index for each unique combination of deflection parameters is computed by forming the first time derivative of the NEO's state vector at the instant in time when the deflection has been applied, as shown in Eq. (7).

$$\dot{\vec{R}}_{NEO}\left(t_{DEF+}\right) = \left\{ \begin{bmatrix} \vec{v}_{NEO}\left(t_{DEF+}\right) \end{bmatrix} \\ \begin{bmatrix} \ddot{\vec{r}}_{NEO}\left(t_{DEF-}\right) \end{bmatrix} \right\} \tag{7}$$

Note that the deflected NEO velocity in the state vector specification is computed according to Eq. (3). The second time derivative of the NEO's position vector is simply the acceleration acting upon its center of mass as computed by whatever force model is being utilized and does not depend on any deflection parameters other than t_{DEF}.

Next, the state vector derivative in Eq. (7) is integrated forward in time from time t_{DEF+} to time t_{CA+} via whatever numerical integration scheme is being utilized, as shown in Eq. (8).

$$\begin{bmatrix} \vec{R}_{NEO}\left(t\right) \end{bmatrix}_{DEF} = \int_{t_{DEF+}}^{t_{CA+}} \dot{\vec{R}}_{NEO}\left(t_{DEF+}\right) dt \tag{8}$$

The position portion of the resulting NEO state time history is then used to compute the minimum distance between the NEO and Earth for the deflected NEO trajectory as shown in Eq. (9).

$$\begin{bmatrix} \Delta r_{MIN} \end{bmatrix}_{DEF} = \min\left(\left\| \begin{bmatrix} \vec{r}_{NEO}\left(t\right) \end{bmatrix}_{DEF} - \vec{r}_{EARTH}\left(t\right) \right\| \right) \tag{9}$$

Finally, the result of Eq. (9) is used in Eq. (2) to compute the performance index value corresponding to the combination of deflection parameters used. As all the combinations of deflection parameters are sampled in turn, a vector of performance index solutions, $\vec{P}$, to which the list of combinations map is formed.

The two conditions for the optimal solution are that P is maximized overall *and* that the condition of non-collision holds over the time interval spanning the time immediately following deflection up to a time subsequent to the closest approach of the NEO to Earth on the deflected trajectory, denoted by $\begin{bmatrix} t_{CA+} \end{bmatrix}_{DEF}$, which is generally close to but not the same as the time of collision or close approach on the undeflected trajectory. Neither condition is sufficient alone though both are necessary. In combination they are necessary and sufficient.

Future work includes determining how to mathematically incorporate an additional condition into the performance index: that the NEO not be deflected into a gravitational keyhole, which would cause the NEO to return to strike Earth some number of years later. However, even if the NEO were to be deflected onto such a trajectory, at least we avert the first collision and are able to prevent the second collision with a second deflection mission.

Equation (10) expresses the first necessary optimization condition and Eq. (11) expresses the second necessary optimization condition. The time interval over which Eq. (11) must be satisfied is given in Eq. (12).

$$P_{OPT} = \max(\vec{P}) \tag{10}$$

$$[\Delta r(t)]_{DEF} > (R_{EARTH} + M_{SAFE}) \tag{11}$$

$$t_{DEF+} \leq t \leq [t_{CA+}]_{DEF} \tag{12}$$

Following from the optimization condition of Eq. (10), and requiring that Eq. (11) is satisfied over the interval given in Eq. (12), Eq. (13) expresses the definition of the optimal deflection solution vector itself.

$$\{t_{DEF}, \Delta v, \alpha, \delta\}_{OPT} \ni P = P_{MAX} \tag{13}$$

Equation (13) states that the optimal solution vector is the combination of deflection time, applied impulse magnitude, azimuth angle, and elevation angle that globally maximizes the performance index.

Given the fact that there is no analytical solution to the N-body gravity equations of motion and that the force model used may also include solar radiation pressure and the Yarkovsky effect, a direct analytical optimization is not deemed feasible for this problem. Direct numerical optimization schemes may be able to handle the problem, however, and further research will examine various numerical optimization schemes in the hope of finding one that handles the problem efficiently.

The deflection parameter sampling method offers two advantages over direct methods. First, it is guaranteed to identify the optimal solution provided the sampling resolutions are fine enough. Second, it automatically provides the data required to quantify the sensitivity of the achieved deflection to deviations from the optimal solution. This information is crucial for determining the required precision that must be exercised during a deflection mission, or conversely, by how much unanticipated errors in the application of the deflection will degrade the achieved deflection

The disadvantage to the sampling method is that is very computationally intensive. Future research into numerical optimization algorithms applicable to this problem should alleviate the computational intensity issue. One final advantage of the methods presented herein is that they are crucial for validating any direct numerical optimization scheme and they also can compliment a direct optimization by providing sensitivity data local to the optimal solution in the design parameter space.

The computational intensity of the sampling method is mitigated by the fact that the set of deflection parameters to sample can be partitioned easily and the algorithm is readily parallelized since each evaluation of the performance index is independent of all other evaluations, allowing the calculations to be completed rapidly on a computing cluster or other distributed computing network.

The algorithm presented herein will be upgraded to treat the case of optimizing a NEO deflection using N impulses, that is, the application of multiple discrete impulses to the NEO at successive times rather than a single impulse, in future research efforts. This will then be extended to the case of continuous, rather than impulsive, deflection. In this case a (necessarily) small thrust is applied to the NEO over some time duration and it is necessary to optimize the orientation of the applied thrust vector over time as well as the on-off sequence for the thruster; that is required because of the NEO's intrinsic spin state.

The penultimate optimal NEO deflection system incorporates all aspects of the overall mission and produces a complete mission design as output given a wide range of high-level requirements and scenario definition data as input. Such a system will also draw upon an integrated database of mission equipment, including launch vehicles, transit and maneuvering thrusters, and deflection devices. The software system will make no a priori assumptions and instead allow the optimal overall mission design to be computed with only logistical constraints applied. A variety of algorithms may be employed here. For example, a genetic algorithm could be used to literally evolve optimal NEO deflection missions.

If the holistic NEO deflection mission optimization system is designed in a very general manner, it can then be further generalized and extended such that it becomes a general optimal spacecraft mission design system that, given high-level requirements and mission objectives as input, produces an optimal end-to-end mission design from launch to mission conclusion. The system may also produce a entire set of mission designs, including the absolute optimal (assuming that there is a global optimal in the overall design space), that satisfy the mission requirements. This mission design system would be an invaluable aerospace engineering tool. It is an excellent example of a very general and powerful design tool evolving from the NEO deflection research effort and is a strongly recommended technology development path.

1. Optimal Solution Trends

It is intuitive and verified in Ref. 1 that earlier deflections generally perform better than later ones. The time of deflection is generally selectable, within the logistical constraints of a particular hazardous NEO scenario (e.g., launch windows, which are a function of orbital mechanics) and within the constraints of the launch/thruster technology of the era.

Also, increasing the magnitude of the velocity impulse, when properly applied, will increase the achieved deflection. However, the cumulative effect of multiple velocity impulses is not known (i.e., linear, exponential, logarithmic, etc.). This study attempts to characterize this behavior. Note that in a given NEO deflection scenario, the magnitude of the applied velocity change is strictly a function of the nature and power of the deflection mechanism, the NEO physical properties, and the physical coupling between the deflection mechanism and the NEO. Thus, for a deflection mechanism and spacecraft, there is an upper limit to the velocity impulse that can be applied to a given NEO.

The orientation of the applied impulse, parameterized by the azimuth and elevation angles, is generally selectable. For instance, a standoff nuclear detonation can be performed by placing the nuclear device anywhere around the NEO prior to detonation. This can be accomplished by rendezvousing with the NEO and then moving to the desired position relative to it. This contrasts with the case of the kinetic impactor, for which the conflicting requirements of minimizing mission fuel requirements and attaining a high relative impact velocity place serious constraints on the directions of the applied impulse. Previous research presented in Ref. 1 indicated that the optimal elevation angle is generally zero, meaning that the optimal deflecting impulse vector always lies in the NEO's orbit plane. Current research has found that this is true in most, but not all, cases.

A well-known method of maximizing the effect of a velocity impulse on an orbiting body applies to NEOs. To maximize the energy change produced by a given velocity impulse, the velocity change should be applied at periapsis, collinear with the velocity vector. This can be seen analytically by examining the specific mechanical energy of the NEO, given in Eq. (14).

$$\varepsilon_{NEO} = \frac{v_{NEO}^2}{2} - \frac{\mu_{SUN}}{r_{NEO}} \tag{14}$$

The result of computing the partial derivative of Eq. (14) with respect to velocity is shown in Eq. (15).

$$\Delta\varepsilon_{NEO} = v_{NEO}\Delta v \tag{15}$$

What is not obvious from Eq. (15) is how much of an advantage is gained by deflecting at perihelion.

IV. NEO Deflection via Nuclear Device

Of all the devices or systems that can impart an impulse to a NEO, a nuclear explosive device offers the highest energy density by at least several orders of magnitude, meaning that a nuclear explosive deflection system of a given mass will have the potential to deliver a much higher Δv than any other device with an equivalent mass. This is extremely important due to the limitations of launch and space propulsion technology and the importance of rendezvousing with a hazardous NEO as quickly as possible.

A nuclear explosive device is best applied to a NEO in a standoff or surface detonation mode. In these modes of operation, the nuclear device is placed at the optimal coordinates relative to the NEO and then detonated. The

neutron radiation from the blast penetrates a thin layer of NEO surface material, perhaps 10 to 20 cm deep, causing this shell of material to vaporize and blow off to zero pressure. The result is an impulsive thrust applied to the NEO's center of mass, causing a velocity impulse, $\Delta \vec{v}$, to be applied to the NEO. An artistic conception of a standoff nuclear detonation is presented in Fig. 9.

Research has been conducted over the past several years to produce models that predict the required yield and hence the mass of a nuclear explosive device required to impart a given velocity increment to a NEO. Holsapple indicates that a 1 Mt nuclear explosive device is required to impart a 1 cm/s velocity increment to a NEO 1 km in mean diameter, at a standoff detonation distance of 23 m from the asteroid's surface[2]. The key parameter is the required NEO momentum change. The mass of the required nuclear device is directly related to the size of the required momentum change. For reference, a 1 Mt nuclear explosive device has a mass of about 1000 kg, well within the capabilities of current launch vehicle and space propulsion technology[3].
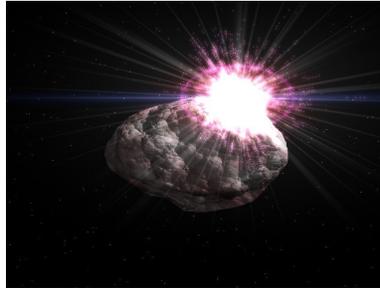
Figure 9. Artistic conception of a standoff nuclear detonation performed on a NEO[*].

Holsapple's work in Ref. 2 shows that placing the nuclear explosive device at the proper distance from the NEO is important to ensure that Δv is maximized. Additionally, in order to achieve the optimal direction for $\Delta \vec{v}$, it is necessary to position the nuclear device not only at the proper distance from the NEO but also at the coordinates relative to the NEO in the RIC frame that yield the optimal direction for $\Delta \vec{v}$. The associated geometry for the case of a spherical NEO is shown in Fig. 10.
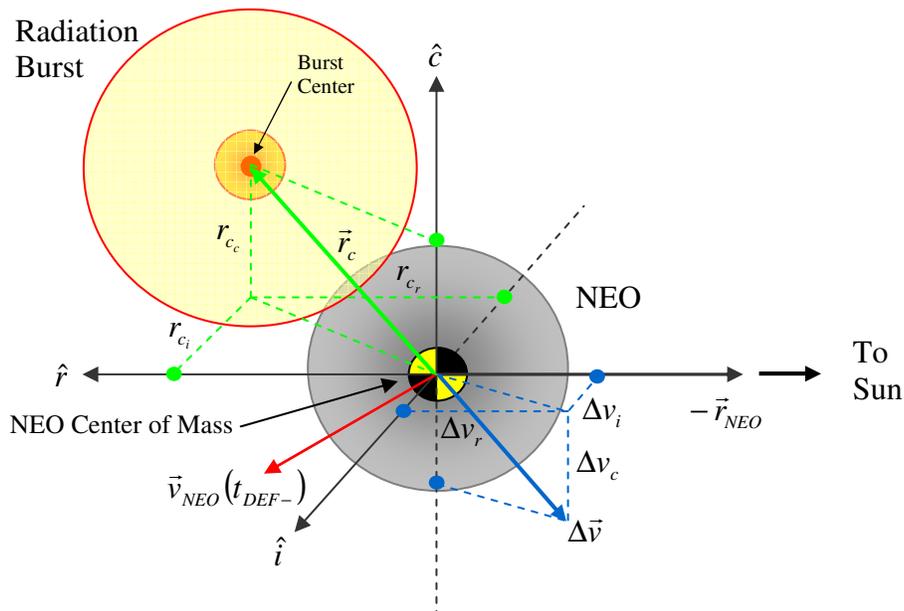

Figure 10. Nuclear device positioning geometry for a standoff nuclear detonation applied to a spherical NEO.

[*] Wilkins, Peter A. Computer rendering of asteroid model and standoff nuclear detonation. (November 2005).

Figure 10 shows that the $\Delta\vec{v}$ resulting from the standoff nuclear detonation will be in the opposite direction of the position vector of the device at the time of detonation, relative to the NEO's center of mass. The optimal coordinates for the device, incorporating the optimal detonation distance and optimal azimuth and elevation angles, the definitions of which are shown in Fig. 6, are readily computed using equations in Ref. 1. While NEOs are not generally spherical and have surface topology that must be accounted for, the spherical case demonstrates the important concept; a more detailed model can be generated that computes the optimal detonation coordinates while accounting for the actual shape and surface topology of a given NEO, and this will be required for actual deployment of nuclear devices for NEO deflection, both to test the technology and utilize it in a true emergency.

As with all technologies, there are advantages and disadvantages associated with the use of nuclear devices as NEO deflection mechanisms. These are summarized in Table 1, along with means of addressing the disadvantages.

Table 1. Advantages, disadvantages, and means of eliminating disadvantages associated with the use of nuclear devices for NEO deflection[4].

Advantages	Disadvantages	Means of Addressing Disadvantages
Most of the required technology is currently available at TRL 9, except for nuclear device payload handling and precision NEO proximity operations.	Not all types of NEOs are susceptible to standoff nuclear detonation; very porous NEOs or "rubble piles" may not be significantly affected.	Testing nuclear devices on harmless NEOs in order to determine which types of NEOs are susceptible and which are not. Testing will also correct our models for the coupling and interaction between a nuclear explosion in space and a NEO. Additionally, repeated testing will lead to more robust models that can provide good predictions of the proper nuclear device to use even if a preliminary science mission to a NEO is not possible.
NEO deflection provides a beneficial use for nuclear explosives.	The coupling and interaction between a nuclear explosion in space and a NEO is unproven.	
The impulsive and vigorous nature of nuclear explosives makes it possible to deflect NEOs with relatively little warning (5 – 10 years).	Proper selection of the nuclear device requires knowledge of the target NEO's physical parameters at a level of detail requiring a preliminary science mission, and such a precursor mission may not be possible for a scenario with low warning time.	
No anchoring of equipment to the NEO's surface is required.	If the launch vehicle explodes while still in Earth's atmosphere, it is possible that some radioactive material could be scattered on Earth.	Nuclear devices have already been designed to not accidentally detonate even if subjected to a launch vehicle explosion. All that remains is to design methods for packaging them within the launch vehicle to minimize or eliminate the risk of radioactive material being scattered should the launch vehicle fail.
The NEO's spin state is not a factor.	There is an international treaty forbidding the detonation of nuclear devices in space.	The appropriate international parties can amend the treaty prohibiting nuclear device detonation in space to allow it for the purpose of NEO deflection device testing and the use of such devices in a true hazardous NEO scenario.
No extended on-orbit operation of equipment is required.		
Nuclear explosives offer the highest energy density of any current or foreseeable practical technology.		

Despite the clear technical reasons for employing nuclear devices as NEO deflection mechanisms, there are those who disagree. Some people believe that using nuclear devices for NEO deflection would be taken advantage of by malicious world leaders as a means to justify further nuclear device stockpiling. There is a very strong argument that this is not true. No world leader would be able to make a case for creating substantially larger nuclear device stockpiles solely for NEO defense purposes because not very many nuclear devices are required for either testing on NEOs or being prepared for an actual hazardous NEO; sufficient nuclear devices exist today. Furthermore, a malicious leader will gain far more public support for nuclear device stockpiling by appealing to the public's fear of another nation, which is readily personified and vilified, rather than trying to incite public fear of NEOs, which are remote distant objects that do not provoke the average person's emotions nearly as much as national pride or fear of terrorism and war do.

More importantly, nuclear devices are not going to disappear simply because some individuals view them as an icon of human aggression and destruction. These devices are tools like any other, and any space faring species, which humans aspire to be, most certainly requires tools that can generate large bursts of energy in the space environment for a variety of non-malicious purposes. In short, nuclear devices are a technology that humanity is going to be forced to learn to live with maturely, regardless of whether we ever use them for NEO deflection.

V. Asteroid Apophis Case Study

Asteroid Apophis, initially designated 2004 MN4, now numbered 99942, was discovered on June 19th, 2004[*]. The initial orbit determination for Apophis indicated that it had a high probability of colliding with Earth in 2029. Subsequent radar observations reduced and eventually eliminated the probability of impact in 2029, but Apophis still has the distinction of being the most apparently dangerous NEO yet discovered.

It is now known that on Friday, April 13th, 2029 at 21:46:13.44 TDB Apophis will closely approach Earth at a distance of approximately 38331.57 km (0.000256 AU), placing the asteroid at an altitude of 31953.44 km, which is 3832.43 km closer to Earth than our geosynchronous satellites. During this close approach event, there is a 2.2×10^{-5} probability (0.0022% chance) that Apophis will pass through a gravitational keyhole approximately 600 m wide[†], causing Apophis to collide with Earth exactly 7 years later, in 2036. The asteroid's estimated physical characteristics and predicted speed and delivered energy for a 2036 impact are presented in Table 2.

Table 2. Apophis physical characteristics and 2036 impact metrics.

	Scientific Units[‡]	Equivalent Intuitive Units
Estimated Mean Diameter	250 m	0.155 miles
Estimated Mass	2.1×10^{10} kg	59350 fully loaded 747 airliners
Estimated 2036 Earth Impact Speed	12.59 km/s	28163 mph
Estimated Earth Impact Energy	400 Mt	20000 Hiroshima bombs (20 kt each)

Apophis is potentially the most hazardous NEO discovered to date. While Apophis is not of sufficient size to have globally catastrophic consequences should it strike Earth, the damage would still be tremendous. An Apophis impact would create tsunamis on the coastlines bordering any ocean struck and cause extremely widespread death and destruction should it strike land near populated areas. There is no doubt that a deflection mission will be sent to Apophis if it is found to be headed towards a 2036 Earth impact.

Apart from the uncertainty regarding whether Apophis will collide with Earth in 2036, there are other unanswered questions. For instance, Earth's gravity might have a disruptive effect on Apophis during the 2029 close approach. In 1992, comet Shoemaker-Levy 9 was torn into a dozens of fragments during a close approach of Jupiter; 21 of the fragments collided with Jupiter 2 years later in 1994[§].

The following sections present an analysis of Apophis rendezvous trajectories and discuss the payload mass deliverable to the asteroid by two different launch vehicle and arrival thruster configurations. This analysis then relates the payload mass to cost. Available launch windows for rendezvous with Apophis between 2008 and 2036

---

[*] http://earn.dlr.de/nea/099942.htm

[†] Email correspondence with Dr. John Junkins, Aerospace Engineering Faculty Member, Texas A&M University.

[‡] http://neo.jpl.nasa.gov/risk/a99942.html

[§] http://en.wikipedia.org/wiki/Comet_Shoemaker-Levy

are identified, followed by a detailed optimal deflection analysis for Apophis. Finally, all of the results are synthesized to generate a brief outline for a campaign of missions to the asteroid.

A. Rendezvous with Apophis

In order to facilitate the optimal deflection analysis, a set of initial conditions for Apophis's state were generated that precisely reproduce the 2029 close approach when integrated forward in time under the influence of the force model chosen for this study. The same initial state is utilized for all trajectory calculations as well. An N-body gravitational force model is used that includes the Sun, Earth, and Apophis, with the Sun fixed at the center of the HCI frame. An Adams method (predictor-corrector) implicit numerical integration scheme with a maximum order of 12, found within the LSODE solver in ODEPACK[*], was used for all state propagations for both trajectory generation and optimal deflection analysis.

The initial state generated for the analyses herein is presented in Table 3, along with the state information at the same epoch as provided by the JPL HORIZONS system for comparison. The data in Table 3 show that the Apophis orbit used here in is slightly different from that found within HORIZONS, as is expected due to the force model utilized herein. This very slight difference does not alter the character of the asteroid's orbit at all and hence the initial conditions generated for this study are quite sufficient for both the trajectory design and optimal deflection analyses.

Table 3. Apophis state information used at the epoch 2454000.5 JD.

Orbital Element	This Case Study	HORIZONS[†]
a (semi-major axis)	0.921932799661088 AU	0.9222630752897020 AU
e (orbital eccentricity)	0.191323254392897	0.1910585040960234
i (orbital inclination)	3.3460887568784°	3.331325583225698°
Ω (Right Ascension of Ascending Node)	204.198400203799°	204.4600025734231°
ω (Argument of Perihelion)	126.405963008497°	126.3955232966237°
M (Mean Anomaly)	82.4540741738348°	84.78650698839441°

Trajectories were computed via Lambert targeting for bringing a spacecraft to rendezvous with Apophis by sampling a space consisting of departure date and time of flight on the rendezvous trajectory. The specifics of this algorithm are expounded upon in other research[5]. The algorithm characterizes all rendezvous trajectories according to the maximum amount of payload mass that can be delivered to the asteroid for a given combination of launch vehicle and arrival thruster. Optimal trajectories are those that deliver the largest payload mass when compared to neighboring trajectories.

Two spacecraft configurations are considered and are summarized in Table 4. The first is a Discovery Class configuration similar to the hardware utilized by the 2001 NEAR-Shoemaker mission to the asteroid Eros. Discovery Class mission criteria established by NASA are that maximum cost of the mission cannot exceed $299 million and the mission must go from concept to launch in no more than 36 months[‡].

The second configuration is a Heavy Lift configuration that uses a Boeing Delta-IV Heavy launch vehicle, one of the most powerful launch systems currently available, and a Pratt & Whitney RL-10 thruster that has a strong performance record and one of the highest specific impulse ratings for contemporary upper stage engines.

---

[*] http://www.netlib.org/odepack/opkd-sum

[†] http://ssd.jpl.nasa.gov/horizons.cgi

[‡] http://solarsystem.nasa.gov/missions/future5.cfm

Table 4. Spacecraft configurations considered for Apophis rendezvous.

Discovery Class		Heavy-Lift	
Launch Vehicle	Rendezvous Thruster	Launch Vehicle	Rendezvous Thruster
Boeing Delta-II-2925-9.5	NEAR[*] (I_{SP} = 313 sec)	Boeing Delta-IV-4050H-19	P&W RL-10 (I_{SP} = 451 sec)

The performance parameters for each spacecraft configuration in Table 4 were obtained and programmed into the trajectory computation software. Figures 11a and 11b show the resulting maximum deliverable payload mass for the two spacecraft configurations as a function of departure date and flight time. The payload masses already account for the fuel expended during the arrival maneuver. There are several clearly advantageous launch windows with one local optimal per advantageous launch window. Large sections of the departure date vs. flight time space are found to be unreachable with the spacecraft configurations considered here (the dark blue regions).

In particular, there is a region of viable departure dates, approximately 1 year wide, centered on each of the optimal departure dates, which are given in Table 5 for the Discovery Class configuration and in Table 6 for the Heavy Lift configuration. The general trend is that the Discovery Class configuration is capable of placing approximately 400 kg on orbit with Apophis while the Heavy Lift configuration is capable of delivering a 4300 to 4400 kg spacecraft. The Discovery Class performance is within expectations as the mass of the NEAR spacecraft was approximately 450 kg. Other spacecraft configurations would deliver overall performance somewhere between the Discovery and Heavy Lift classes discussed here.

(a)   (b)
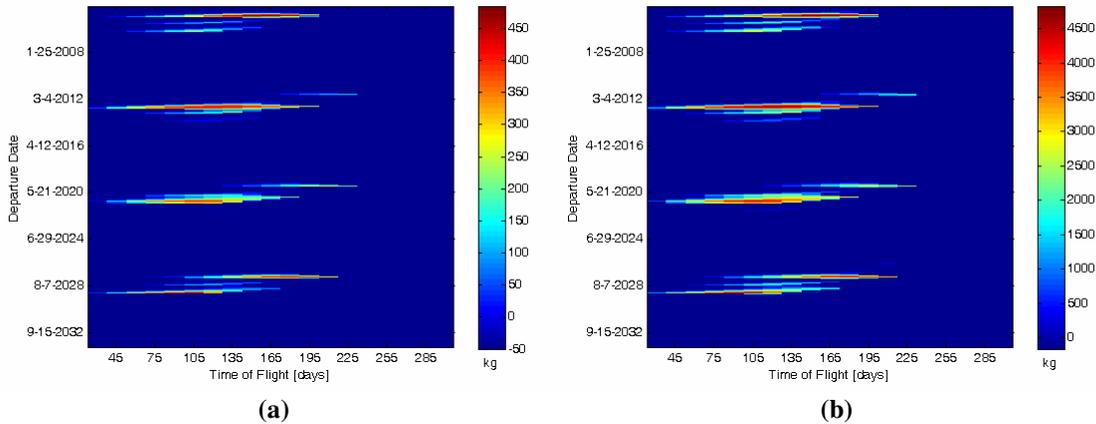
Figure 11. Deliverable payload mass for (a) Discovery Class configuration and (b) Heavy Lift configuration.

There are three particular missions of interest for Apophis. The first is a small and simple orbit determination mission whose sole objective is to determine Apophis's orbit accurately enough to conclusively determine whether Apophis will indeed pass through the 2036 impact keyhole in 2029. This is potentially a very low-mass mission and readily accommodated by the Discovery Class configuration. As an example, an X-band transponder beacon transmitting with only 5 W of power to a 35 m receiving dish on Earth can achieve position accuracy on the order of 100 m and velocity accuracy on the order of 0.1 mm/s at range of up to 2 AU from Earth[6]. The second mission is a combination science and orbit determination mission whose objectives are to perform high-accuracy orbit determination on Apophis and conduct a thorough scientific characterization of the asteroid. The science data would be quite interesting from the point of view of understanding NEOs in general. Moreover, if the orbit determination finds that Apophis is going to pass through the keyhole, then the science data on Apophis's composition and structure will be absolutely crucial to the design of the deflection system deployed against Apophis.

---

[*] The "Discovery Class" profile is meant to match what was used in the 2001 NEAR-Shoemaker mission to the asteroid Eros. The NEAR spacecraft's primary thruster had a specific impulse of 313 seconds and the spacecraft was launched on a Delta-II-7925-8 rocket. The 7925 series has since been re-designated 2925 and the 9.5 ft diameter fairing is the closest currently available fairing to the 8 ft fairing used for the NEAR mission.

Table 5. Maximum delivered payload mass trajectory results for Apophis rendezvous with Discovery Class configuration.

Departure Date	Flight Time, days	Maximum Deliverable Payload Mass, kg
October 7, 2012	120	409.14
February 4, 2021	105	413.59
March 17, 2029	105	445.44

Table 6. Maximum delivered payload mass trajectory results for Apophis rendezvous with Heavy Lift configuration.

Departure Date	Flight Time, days	Maximum Deliverable Payload Mass, kg
October 22, 2012	120	4475.88
February 4, 2021	105	4332.99
March 17, 2029	105	4448.22

There are two very favorable available ranges of launch times for rendezvous with Apophis prior to the 2029 time frame. The first range of favorable launch times is on or around 2012 and the second is on or around 2021. The only favorable launch times between 2029 and 2036 are during 2029, right around the time of close approach.

The trajectory for a characteristic maximum deliverable payload mass rendezvous with Apophis is shown in Fig. 12a, which is specifically for a rendezvous in the 2012 timeframe; the rendezvous trajectories for the other advantageous timeframes look approximately the same and hence are not shown here. The delivered payload mass performance in the 2012 timeframe is shown in Fig. 12b. Note that the advantageous launch opportunities repeat each time that Earth and Apophis are close to each other. The synodic period of the Earth-Aphopis pair is approximately 8 years.

| (a) | (b) |
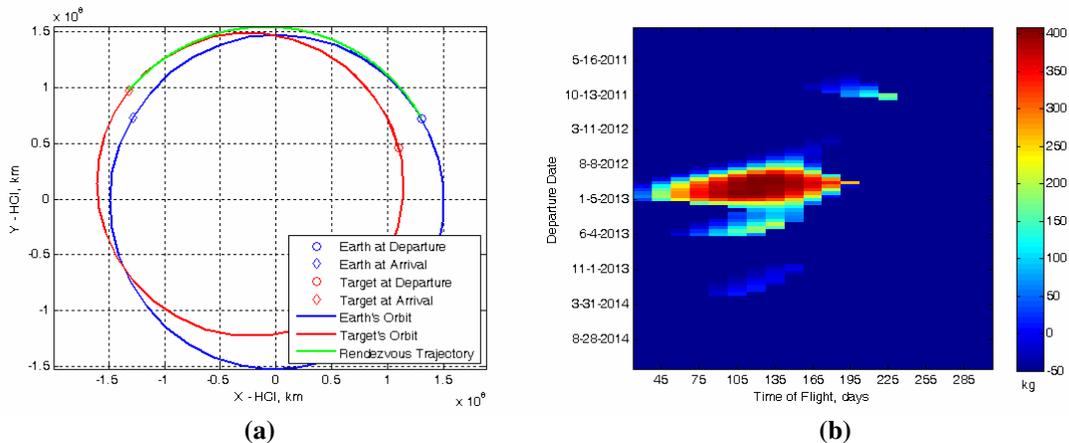
Figure 12. (a) Maximum mass rendezvous with Apophis in 2012 and (b) delivered payload mass to Apophis in the 2012 timeframe as a function of departure date and flight time.

A logical sequence of events is to reconnoiter Apophis in the 2012 timeframe, gathering precise orbit determination data and conducting a thorough scientific characterization of the asteroid. The delivered payload mass numbers in Table 5 for the Discovery Class configuration suggest that such a mission could be performed at or below the cost of the 2001 NEAR-Shoemaker mission, which characterized the asteroid Eros for a Discovery Class budget of approximately $300 million dollars. The 2012 Apophis mission obtains a valuable science data product regardless of whether the asteroid will in fact strike Earth in 2036. The orbit determination segment of the mission would provide sufficient information to determine whether a 2036 impact would actually occur. If a 2036 impact is found to be certain, the 2021 launch window can be used to launch one or more deflectors. If no impact impends, our attention can be focused elsewhere.

Nature, it seems, has provided humanity with a rather straightforward and readily soluble hazardous NEO scenario, yet the 2012 characterization mission has not yet even been planned. It is clear that the world's space agencies have a vested interest in sending science missions to asteroids and comets as we have visited three thus far

and plan to visit more; it seems that, out of all possible target NEOs for science missions, the most threatening NEOs, however small the perceived probability of Earth impact, would be at the top of list of science targets. Since we currently know so little about NEOs in general, there is no reason for Apophis to be considered any less interesting from a scientific standpoint than Itokawa or Eros, both of which have been reconnoitered by science spacecraft.

The current strategy seems to be to wait for more radar observations of Apophis, which will hopefully be available in the 2012-2013 timeframe. It will be unfortunate if these observations indicate a probability of a 2036 impact that is too high to ignore because our ~2012 launch windows will have passed and we cannot easily be on-orbit with Apophis until 2021. This greatly reduces the time interval between the time at which we apply a deflection to Apophis and time of close approach. This delay reduces the optimal deflection performance dramatically.

The current study examines optimal deflection capabilities for Apophis in the pre-2029 era, with the goal of applying an optimal deflection to Apophis pre-2029 that pushes it well clear of the keyhole region, thereby averting a 2036 impact. Should Apophis be allowed to pass through the keyhole and become locked into a 2036 Earth-impacting orbit, we would have to launch a deflection mission between 2029 and 2036. The trajectory analysis data above shows only one advantageous range of departure dates around the March 2029 timeframe. Thus we would essentially be launching immediately prior to Apophis's keyhole passage and rendezvousing shortly after, at which point we would deflect it from a 2036 Earth impact. Future work will perform an optimal deflection analysis for this case.

B. Optimal Deflection Results for Apophis

The approach taken in this study to prevent any possibility of a 2036 collision is to deflect Apophis from passing through the keyhole during 2029, meaning that the times of deflection considered are all prior to April 13th, 2029. Thus the performance index meters the amount by which a given deflection pushes Apophis further away from Earth, and hence further from the keyhole[*], at closest approach. So, to compute the Earth close approach distance for any given "deflection" value presented herein, simply add the "deflection" value to the original close approach distance of 38331 km.

While a wide range of possible times of deflection are considered in order to characterize the overall behavior of the optimal solutions, it is important to note that the available launch windows for Apophis rendezvous discussed previously must be taken into account in order to identify which times of deflection are accessible. Thus the true optimal solution is also a function of available rendezvous trajectories. Deflecting earlier is better, as demonstrated in the data that follows, but this is constrained because the mission has to carry a certain amount of mass of deflection equipment to the NEO and how quickly this mass can be transported to rendezvous is a function of both the technology of the era and the relative orbital dynamics between Earth and the NEO.

The total optimal deflection analysis for Apophis is divided into three cases and the parameters utilized in each case are summarized in Table 7. The specific results of each case are discussed in turn.

Table 7. Summary of optimal deflection analysis parameters for Apophis by case.

	Case 1	Case 2	Case 3
Number of Deflection Times, t_{DEF}	76	25	5
Applied Impulse Magnitudes, Δv	0.1, 1.0, 10.0 cm/s	1.0 cm/s	1.0 cm/s
Azimuth Angles, α	0° to 359°	0° to 359°	0° to 359°
Azimuth Resolution, α_{RES}	1°	3°	3°
Elevation Angles, δ	0°	-90° to 90°	-90° to 90°
Elevation Resolution, δ_{RES}	N/A	15°	15°

---

[*] Technically, pushing the asteroid closer to Earth at closest approach can be effective for collision avoidance, provided the asteroid misses the keyhole. However, we still do not consider deflections that push a hazardous NEO *closer* to Earth to be desirable.

In all figures that present optimal deflection results in what follows, please note that all data points that correspond to Apophis perihelion passage are denoted by blue markers.

1. Case 1 Results

Apophis passes through its perihelion 25 times prior to the 2029 close approach, and each of these times are sampled as deflection times in Case 1. Case 1 also samples two evenly spaced times of deflection before and after each perihelion passage, when the asteroid is at true anomalies of 135° and 222°. The only exceptions to this are the first two times of deflection, at which Apophis's true anomalies are 104° and 189°. All of these true anomaly values at deflection times are shown in Fig. 13. Thus Case 1 samples a total of 76 times of deflection, beginning on September 22, 2006 (22.56 years before close approach) and ending on November 25, 2028 (140 days before close approach). The September 2006 deflection is intended to show by how much Apophis could have been deflected had we sent a deflection mission during a February 2006 launch window, illustrating what would have been possible if humanity had become proficient at deflecting NEOs prior to discovering Apophis. The azimuth angle spans 0° to 359° at a 1° resolution and the elevation angle is fixed at 0°. Three applied velocity impulse magnitudes are sampled, 0.1, 1, and 10 cm/s. This leads to a total of 82080 deflections sampled in Case 1. Interestingly, 1819 out of the 82080 deflections (2.2%) actually cause Apophis to collide with Earth in 2029. The applied impulse magnitude for all of the 1819 collision cases was 10 cm/s. These 1819 inadvertent collision cases are collectively considered to be an inadmissible region of the deflection parameter space.
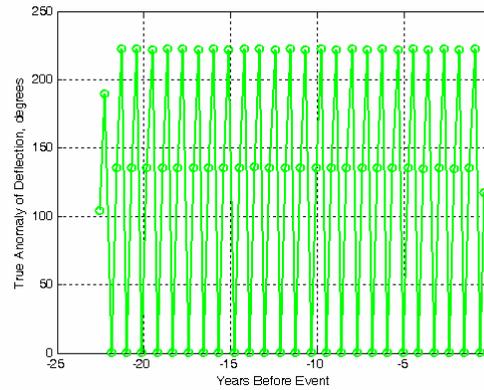
Figure 13. True anomalies at each time of deflection for Case 1.

Figures 14a, 14b, and 14c show the optimal deflection as a function of time for applied impulse magnitudes of 0.1, 1, and 10 cm/s, respectively. Several key features are evident in these data plots. First, comparing all three plots makes it clear that there is a fine structure to the data that increases in uniformity as the magnitude of the applied impulse increases. In fact, the breakdown of this fine structure is readily apparent in Fig. 14a, which shows the optimal deflection results for an applied impulse magnitude of 0.1 cm/s, a very tiny impulse.
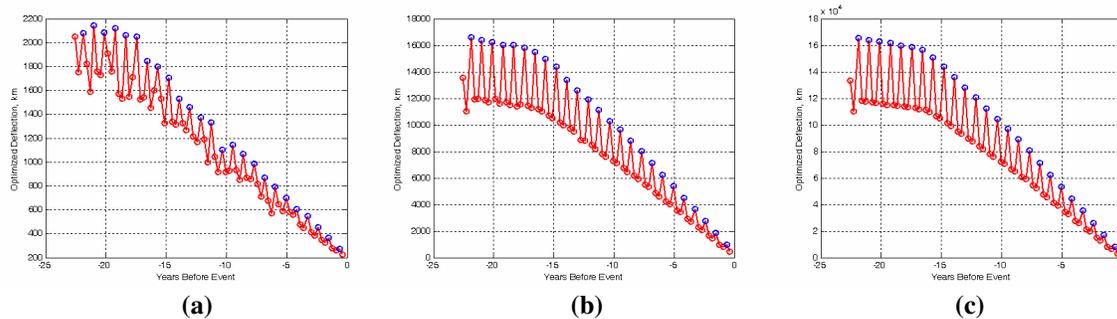

| (a) | (b) | (c) |

Figure 14. Optimal deflection vs. time of deflection for (a) 0.1 cm/s, (b) 1 cm/s, and (c) 10 cm/s.

This breakdown in structure with decreased applied impulse magnitude makes sense because as the impulse magnitude decreases it becomes more and more of a mere perturbation that does not have enough power to compete with the force fields that dominate the NEO's motion.

Because of the breakdown in fine structure for the 0.1 cm/s data, the second interesting feature only manifests in the data for 1 and 10 cm/s applied impulse magnitudes. The feature, seen in Figs. 14b and 14c, is that there are two slopes followed by the optimal deflection values as they linearly decrease with decreasing time until close approach. The inflection point where the slope changes is at approximately 15 years before close approach for both the 1 an 10 cm/s data sets, and the cause for this change in slope is not known at this time but will be investigated in further studies.

Finally, the optimal deflection vs. time of deflection data for all three impulse magnitudes clearly demonstrate that deflections applied at perihelion significantly outperform deflections applied far from perihelion, and the degree to which the perihelion deflection outperforms a deflection applied at another time is directly dependent on the angular distance from perihelion at the other time. This validates the prediction of Eq. (15) that perihelion deflections are the most advantageous and matches the previous findings in Ref. 1.

Figures 15a, 15b, and 15c all show the optimal velocity angle as a function of deflection time for applied impulse magnitudes of 0.1, 1, and 10 cm/s, respectively. All three figures further demonstrate the breakdown in structure as the applied impulse magnitude decreases. The optimal velocity angles for an applied impulse of 0.1 cm/s only track the NEO's velocity direction loosely, with many excursions out to approximately 15° and some out to more than 30°, whereas the optimal velocity angles for impulses of 1 and 10 cm/s track the NEO velocity direction much more closely. Moreover, the 10 cm/s impulse optimal velocity angles track the NEO velocity direction almost twice as tightly as the 1 cm/s optimal velocity angles do.
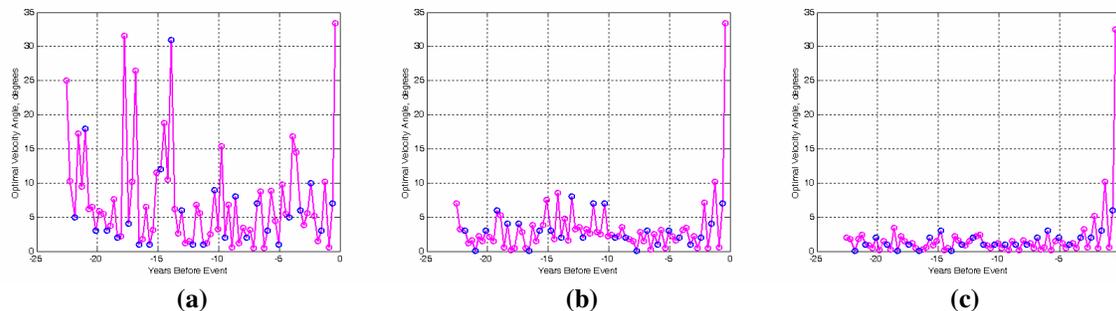

| (a) | (b) | (c) |

Figure 15. Optimal velocity angle vs. time of deflection for (a) 0.1 cm/s, (b) 1 cm/s, and (c) 10 cm/s.

The one optimal velocity angle trend that all three impulse magnitudes have in common is the tendency to begin deviating from the NEO's velocity direction sharply as the time interval between the time of deflection and the time close approach becomes small. In fact, it is very clear in Figs. 15b and 15c that there is a critical transition point at which the optimal velocity angle goes from being approximately 10° to just over 30°. The cause and nature of this transition point is currently unknown and will be the subject of future research. Figures 16a, 16b, and 16c all demonstrate the same trends in terms of optimal azimuth angle as a function of deflection time.
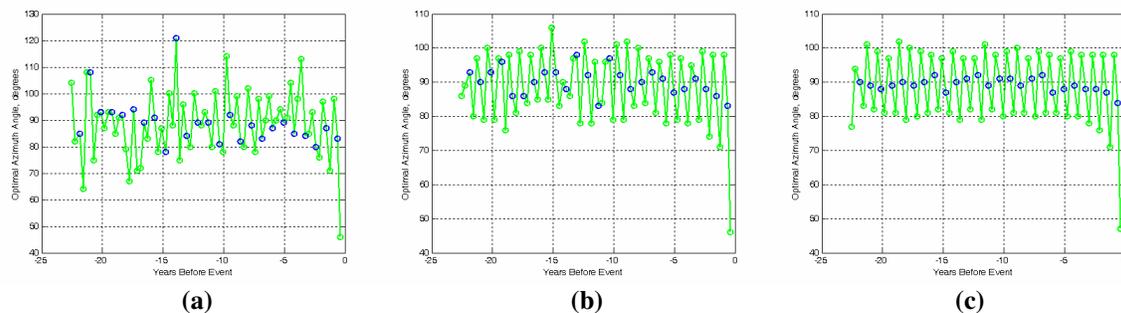

| (a) | (b) | (c) |

Figure 16. Optimal azimuth angle vs. time of deflection for (a) 0.1 cm/s, (b) 1 cm/s, and (c) 10 cm/s.

One of the key advantages to the deflection parameter sampling method for optimization utilized here is that data on the sensitivity of the achieved deflection to deviations from the optimal solution is readily available while it is not

available at all from a direct numerical optimization scheme. Sensitivity results are presented in Figs. 17a, 17b, and 17c for 0.1, 1, and 10 cm/s, respectively. These results show the range in azimuth angle that still yields 95% of the optimal deflection. Again, the breakdown with decreasing impulse magnitude is apparent by noting that the range of 95% optimal azimuth angles varies largely throughout deflection time space for a 0.1 cm/s impulse but is mostly
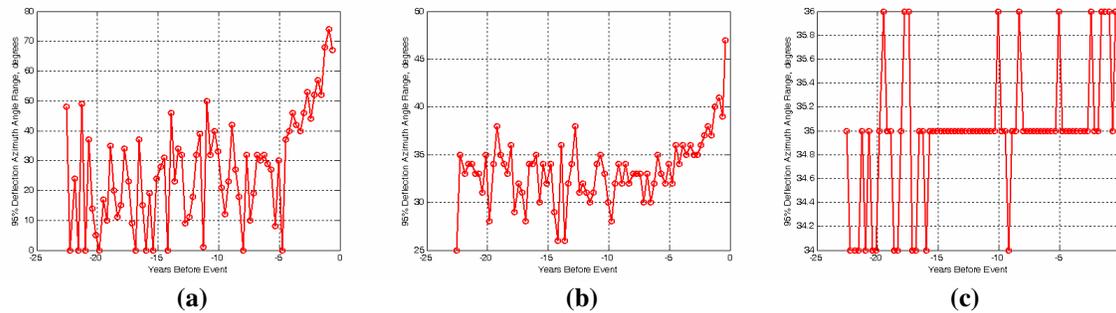

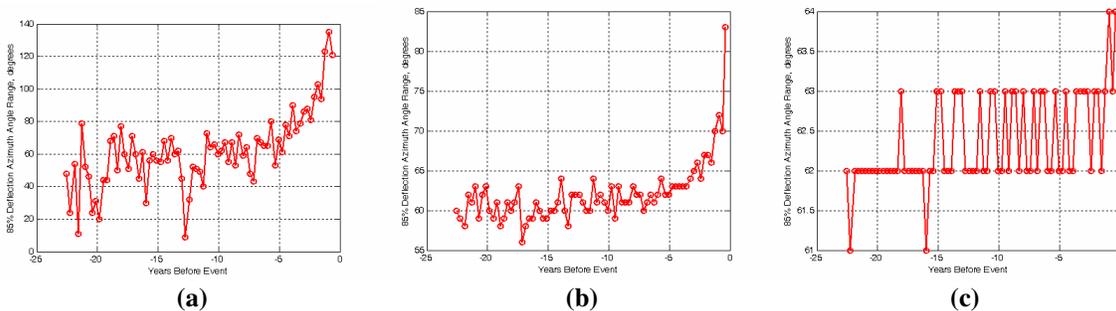| (a) | (b) | (c) |

Figure 17. Azimuth angle range for 95% of optimal deflection magnitude vs. time of deflection for (a) 0.1 cm/s, (b) 1 cm/s, and (c) 10 cm/s.

constrained to between 25° and 37° for 1 cm/s and is even more tightly constrained to between 34° and 36° for 10 cm/s. Note also that while the 95% optimal azimuth angle range begins to increase significantly as the time interval between deflection and close approach becomes small in both the 0.1 and 1 cm/s cases, there is no such increase for the 10 cm/s impulse. Figures 18a thru c and 19a thru c present the 90% and 85% optimal azimuth angle range data, respectively, and demonstrate the same trends as the 95% data. The primary difference is that the size of the azimuth angle ranges obviously increases since the percentage tolerances are looser (90 and 85%).

| (a) | (b) | (c) |
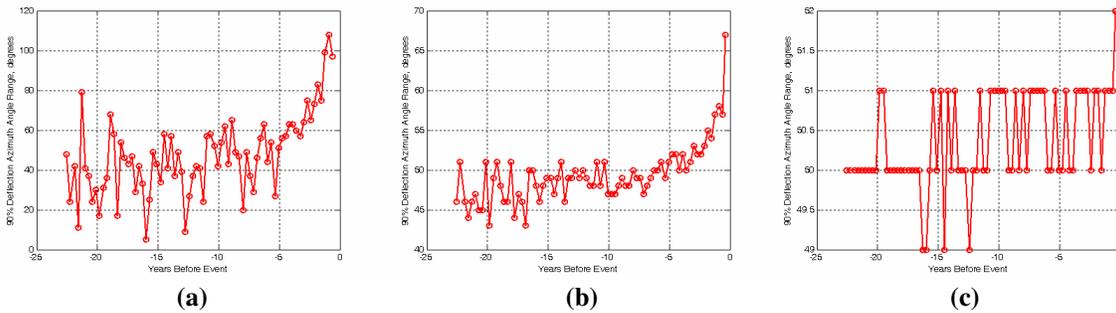
Figure 18. Azimuth angle range for 90% of optimal deflection magnitude vs. time of deflection for (a) 0.1 cm/s, (b) 1 cm/s, and (c) 10 cm/s.

| (a) | (b) | (c) |

Figure 19. Azimuth angle range for 85% of optimal deflection magnitude vs. time of deflection for (a) 0.1 cm/s, (b) 1 cm/s, and (c) 10 cm/s.

Figure 20 presents the performance index surface in impulse magnitude vs. deflection time space. The oscillatory nature of the optimal deflection between perihelion and other true anomaly values can be seen, as well as

the general decrease in optimal deflection magnitude as the time interval between deflection and close approach decreases; the inflection point in the slope is even mostly visible.

The primary feature of interest in Fig. 20 is that the optimal deflection appears to decrease nearly linearly with decreasing applied impulse magnitude, with no finer structure to the behavior. This feature can be seen quantitatively by comparing the optimal deflection values in Figs. 14a, 14b, and 14c; it is clear that a factor of 10 increase in applied impulse magnitude causes the optimal deflection to increase by a factor of almost exactly 10. Furthermore, the optimal deflection values all tend towards zero at the time of close approach and span the same amount of deflection time space, meaning that the higher the magnitude of the applied impulse, the steeper the slope of the decrease in optimal deflection with respect to decreasing time interval between deflection time and time of close approach. This feature is readily apparent in Fig. 20 and can be deduced by comparing Figs. 14a, 14b, and 14c.
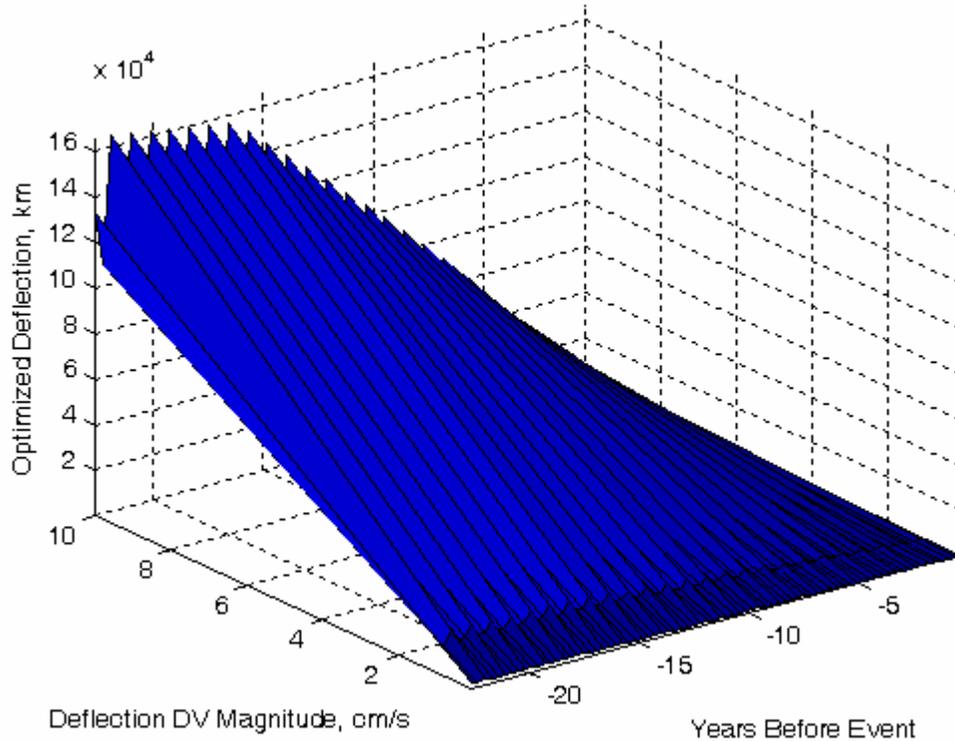
Figure 20. Optimized deflection as a function of both applied impulse magnitude and time of deflection.

2. Case 2 Results

Case 2 samples 25 times of deflection corresponding to each of the 25 perihelion passages that Apophis makes between September 22, 2006 and the April 13, 2029 Earth close approach. The final deflection time sampled is 227 days prior to the close approach. The applied impulse magnitude for each deflection is 1 cm/s and the azimuth angles sampled range from 0° to 359° at a 3° resolution while the elevation angles sampled range from -90° to 90° at a 15° resolution.

The optimal elevation angle was found to always be 0°, as expected, and the optimal azimuth and velocity angles are such that the applied impulse vector tends to track NEO's instantaneous velocity direction to within several degrees, also as expected. The key result of Case 2 is confirmation that the optimally oriented applied impulse vector lies in the NEO's orbit plane, which is consistent with intuition and previous research results presented in Ref. 1..

Sample results are presented for three of the sampled deflection times, 10.37, 9.48, and 8.59 years prior to the 2029 close approach event. The results for these three times are completely representative of the results for all other sampled times of deflection in Case 2. These particular three times of deflection are presented because they represent the deflection achievable by a deflection mission launched to Apophis in the 2021 timeframe. Figure 21a

shows that the optimal available deflection for a 1 cm/s impulse ranges from approximately 10500 km to 9000 km and Fig. 21b indicates that the optimal applied impulse orientation tracks the NEO's instantaneous velocity direction to within approximately 3° to 6°.
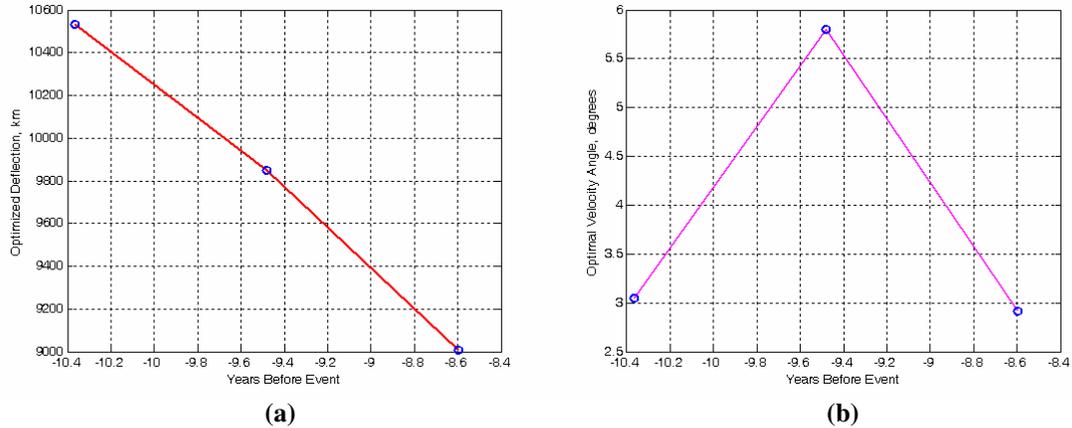

(a)   **(b)**

Figure 21. (a) Optimal deflection magnitude and (b) optimal velocity angle as a function of time of deflection.

The results for the sensitivity of the achieved deflection to deviations from the optimal solution were found to be the same for all three times of deflection shown here and these results are summarized in Table 8. Note that the overall trends for the sensitivities were already presented over the entire deflection time space in Case 1 and hence are not repeated here.

Table 8. Achieved deflection sensitivity to deviations from the optimal solution at 10.37 years before close approach.

	Achieved Deflection	Azimuth Range	Elevation Range
95% of Optimal	10007.36 km	33°	30°
90% of Optimal	9480.66 km	48°	30°
85% of Optimal	8953.95 km	60°	60°

Figures 22a and 22b show the optimal azimuth and elevation angles, respectively, for each time of deflection. The optimal elevation angle is clearly always 0° while the azimuth angle corresponds to the tracking of the instantaneous NEO velocity direction by the optimal applied impulse vector, as discussed previously.
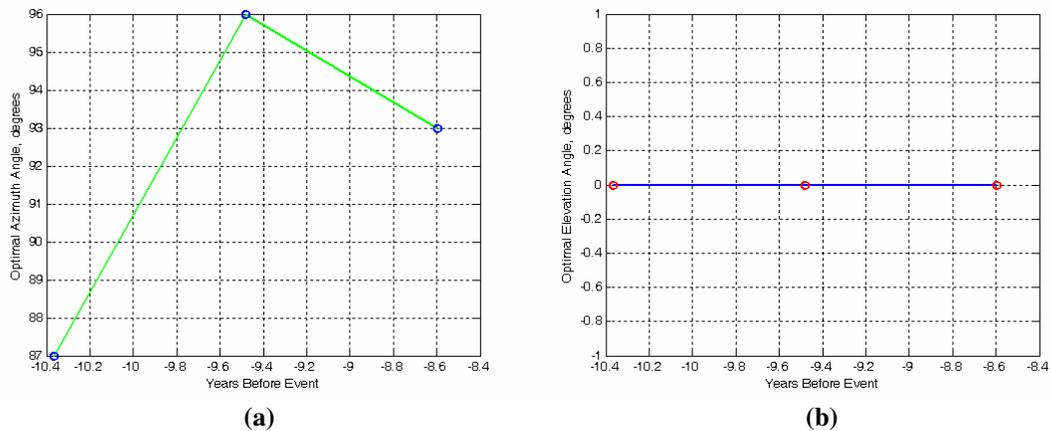

(a)   **(b)**

Figure 22. (a) Optimal azimuth angle and (b) optimal elevation angle as a function of time of deflection.

Figures 23a and 23b show the azimuth-elevation space performance index surface and corresponding three-dimensional plot of the optimal applied impulse vector and the NEO's instantaneous velocity vector for one of the times of deflection in Case 2. Only these figures are provided because they are of the same character as all other such figures for Case 2 data.
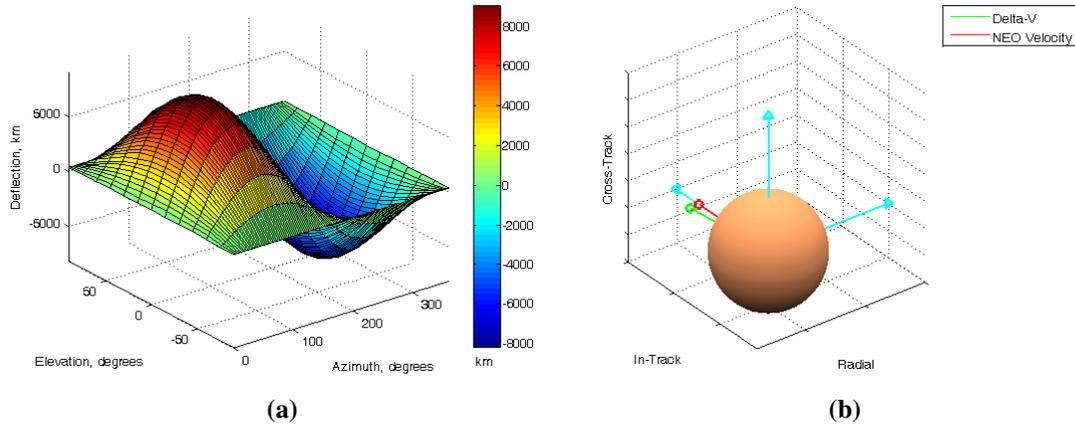

(a)   (b)

Figure 23. (a) Azimuth-elevation space performance index surface and (b) three-dimensional plot of applied impulse vector and NEO velocity vector, both at the time of deflection.

3. Case 3 Results

For Case 3 the magnitude of the applied impulse vector is 1 cm/s and five times of deflection are sampled, 6.12, 4.68, 3.36, 1.92, and 0.6 months prior to the April 13th, 2029 close approach. During these times Apophis's true anomaly changes from approximately 65° to 218°.

Figures 24a and 24b show the optimal deflection magnitude and optimal velocity angle, respectively, at each time of deflection. The optimal deflection magnitude decreases non-linearly and crosses zero between the second and third time of deflection. This marks a transition point for which the maximum value of the performance index is less than zero, meaning that even the optimal deflection pushes the NEO closer to Earth rather than further away. From the point of view of steering the NEO clear of the keyhole this may be just as effective as a positive performance index value of the same magnitude, though we generally consider negative performance index values as mapping to inadmissible regions of the deflection parameter space. Furthermore, the performance index is not designed to recognize that, for the special case of pushing away from a keyhole, the sign of the performance index does not matter, only the magnitude.
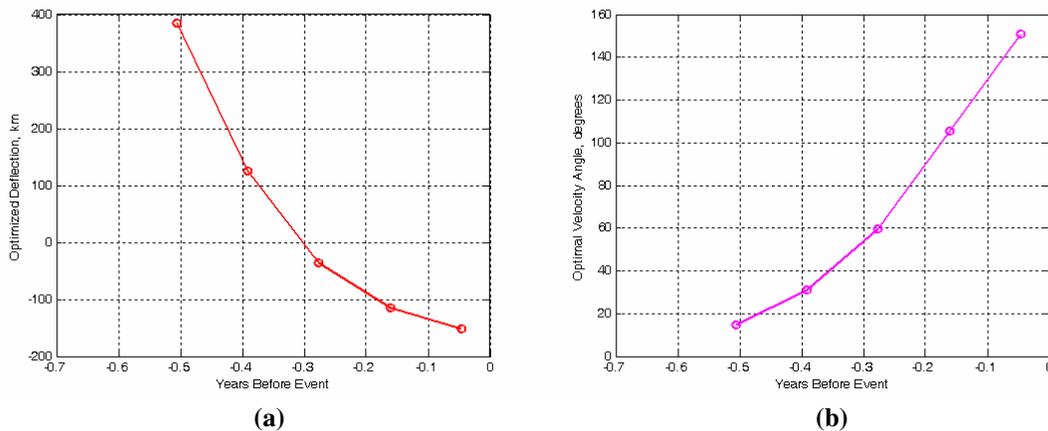

(a)   (b)

Figure 24. (a) Optimal deflection magnitude and (b) optimal velocity angle as a function of time of deflection.

Note that in Fig. 24b the optimal velocity angle changes rapidly from being in the vicinity of the NEO's velocity direction to being mostly radial and then moves towards the direction opposite the NEO's velocity direction. Additionally, Fig. 25a shows a corresponding evolution of the azimuth angle. Furthermore, Fig. 25b shows that the

optimal elevation angle transitions from being zero to being 15° up out of the NEO's orbit plane for the last two times of deflection, which are 1.92 and 0.6 months prior to the close approach.
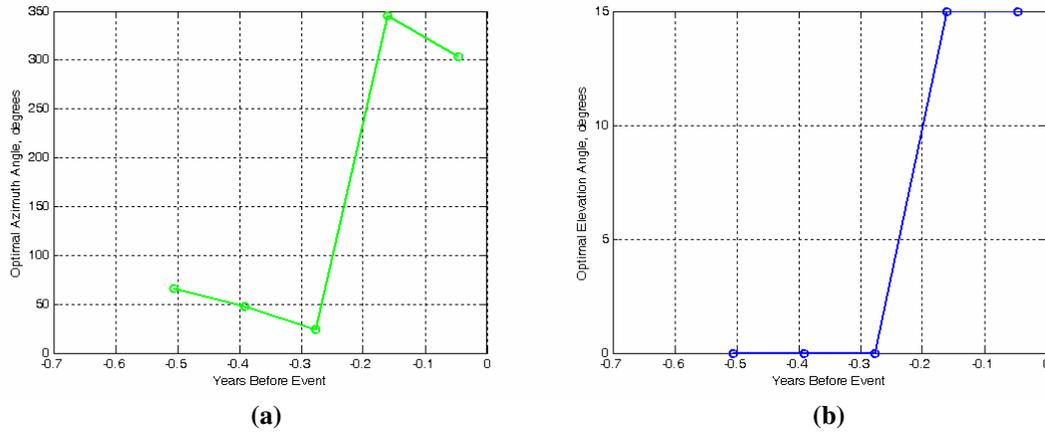

(a)   (b)

Figure 25. (a) Optimal azimuth angle and (b) optimal elevation angle as a function of time of deflection.

This is particularly significant because the optimal elevation angle was found to be 0° for all prior times of deflection. Thus we have discovered that there is a critical point in the deflection parameter space, particularly along the deflection time dimension, for which the optimal elevation angle is non-zero, but only when the time interval between the time of deflection and time of close approach is very, very small. Formulating an explanation for this phenomenon that is consistent with the system dynamics will be the topic of future research. Figures 26a and 26b show the complete azimuth-elevation space performance index surfaces at 6.12 months and 0.6 months prior to close approach, respectively.
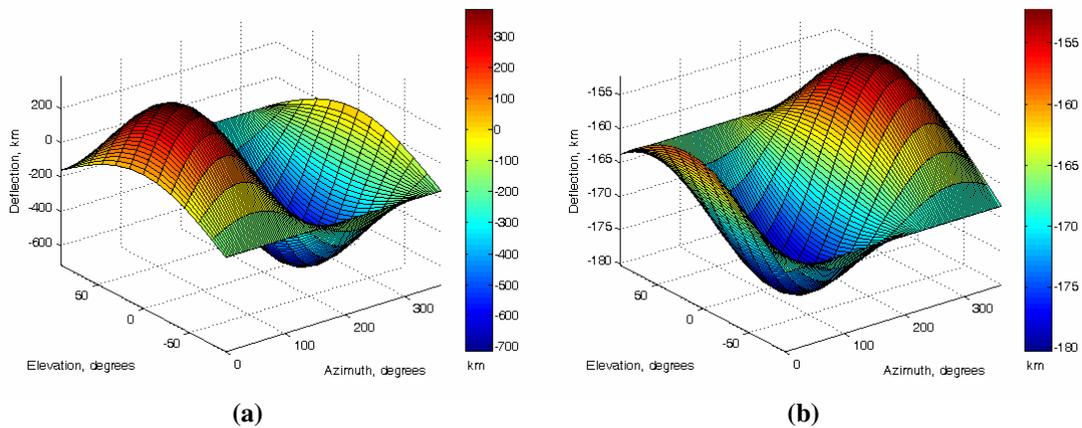

(a)   (b)

Figure 26. Azimuth-elevation space performance index surface at (a) 6.12 months and (b) 0.6 months before close approach.

Figures 26a and 26b clearly show the azimuth angle transition though the elevation angle transition is not as readily visible. However, Figs. 27a and 27b show both the azimuth and elevation angle transitions clearly. In particular, Fig. 27b shows the optimal impulse vector pointing up out of the NEO's orbit plane (Radial-In-Track plane) and tending towards opposing the NEO velocity direction.
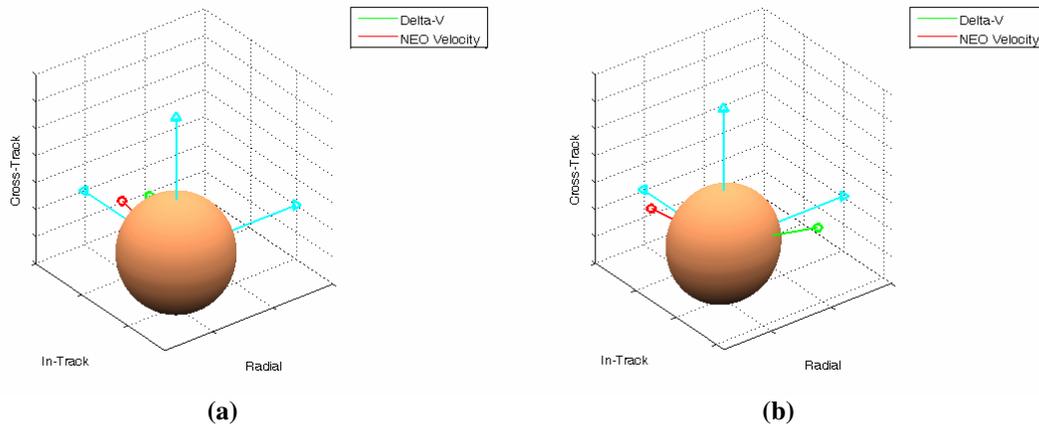
Figure 27. Three-dimensional plot of applied impulse vector and NEO velocity vector at (a) 6.12 months and (b) 0.6 months before close approach.

C. Summary of Apophis Response Mission Design

Based upon the mission design architecture presented in Fig. 2 and the results of this study, we recommend a campaign of missions to Apophis that includes a preliminary science and orbit determination sent to Apophis in the 2012 timeframe. The NEAR spacecraft had a mass of 487 kg and was capable of providing excellent characterization of the asteroid Eros. Since our preliminary trajectory design results for Apophis indicate that a Discovery Class type of mission can deliver around 400 kg to Apophis in 2012, it is very likely that detailed trajectory optimization can increase this performance. Hence, a Discovery Class reconnaissance mission to Apophis in the 2012 timeframe is recommended for the purposes of accurately determining Apophis's orbit and providing a comprehensive scientific data product on the asteroid's physical nature.

If the orbit determination indicates that there is no possibility of Apophis passing through the 2036 impact keyhole during the 2029 close approach, then no further missions are required and we will have gathered a valuable science data product and at the same time increased our NEO response mission proficiency. However, if accurate orbit determination shows that Apophis will definitely pass through the keyhole in 2029 or even have some chance of doing so, then a follow-up deflection mission is required.

Our preliminary trajectory design results indicate that the best time to launch a follow-up deflection mission is in the 2021 timeframe. Given the launch date and nominal flight time, this allows the deflection to be applied to Apophis at the perihelion passage occurring approximately 7.7 years prior to the 2029 close approach, and so the data for this time of deflection will be referenced from Figs. 14a, 14b, and 14c.

The 2021 deflection mission to Apophis has to adopt one of two strategies. The first strategy is to deflect Apophis by the maximum amount possible, in keeping with the philosophy that pushing the asteroid as far away from Earth as possible is the safest course of action. The second strategy is to deflect Apophis just enough to steer it clear of the 2036 keyhole. Since the keyhole is only ~ 600 m wide and even the smallest deflections presented herein (1 mm/s) are in the hundreds of km, this implies that only a very small impulse needs to be applied to Apophis in this case, perhaps a tiny fraction of 1 mm/s. Note that the applied impulse magnitude must be sufficient to clear the keyhole region by a safe margin, and the size of this safe margin has not yet been determined.

The data acquired in 2012 on Apophis's physical nature will influence the deflection mechanism chosen. For instance, if Apophis is either highly porous or a complete rubble pile, we may not choose to employ a nuclear device against it. In this case we might forgo deflection and attempt to bury a nuclear explosive within Apophis and blast it apart, a procedure which is beyond the scope of this work. So we will assume here that Apophis is susceptible to a nuclear device for the purpose of deflection. Note that in this case Apophis would also be susceptible to a kinetic impactor. While the kinetic impactor has a much, much lower energy density than a nuclear device, we have already prototyped kinetic impactor technology during the Deep Impact mission to comet Tempel 1 and it may not be prudent to employ nuclear detonation for the first time ever on an asteroid that is going to come so close to our planet even after the deflection. Nuclear devices should first be tested on harmless NEOs to characterize the expected performance and this has not yet been done, nor is it likely to be done prior to a 2021 deflection mission to Apophis. Here we summarize the potential results for using either a nuclear device or a kinetic impactor on Apophis in 2021.

1.Standoff Nuclear Detonation Deflection of Apophis

Assuming that a Δv of 1 cm/s is achievable with a nuclear explosive device and this impulse would not undesirably disrupt Apophis, Fig. 14b indicates that Apophis can be deflected by 8000 km after a 2021 timeframe rendezvous and subsequent nuclear detonation occurring at the Apophis perihelion passage 7.7 years prior to close approach. Since a 1 Mt device is estimated to be required for a 1 km wide asteroid and Apophis is only a quarter of that size at 250 m, a much smaller nuclear device would theoretically be required since the mass of the asteroid scales down exponentially with decreased diameter. Table 6 shows that the Heavy Lift configuration can deliver around 4300 kg in the 2021 timeframe, and Table 5 shows that the Discovery Class configuration can deliver around 400 kg. If the required nuclear device is small enough, the Discovery Class configuration might suffice, but the Heavy Lift configuration can certainly handle it since even the 1 Mt device has a mass of only about 1000 kg. Further calculations are required to estimate the size of the nuclear device required to impart a 1 cm/s impulse to Apophis.

It is possible that Apophis will be able to have an impulse imparted to it by the nuclear device that is larger than 1 cm/s without danger of disrupting the asteroid undesirably. If so, the achieved deflection is even greater. For reference, Fig. 14c shows that Apophis can be deflected by 80000 km with a 10 cm/s impulse, increasing the 2029 close approach distance to nearly 120000 km, which is a much more comfortable distance for Earth.

On the other hand, if it is only desired to deflect Apophis just clear of the keyhole, including a margin of safety, a very small nuclear device may suffice since an imparted impulse of less than 1 mm/s is required. The keyhole is ~ 600 m in size and Fig. 14a shows that a 1 mm/s impulse applied at the perihelion passage 7.7 years before close approach deflects Apophis by about 1000 km. This implies that an impulse only a small fraction of 1 mm/s would steer Apophis away from the keyhole by a few thousands of meters. This approach might only require a very small nuclear device and be easily serviceable by a Discovery Class mission.

2. Kinetic Impactor Deflection of Apophis

A Δv of at least 1 mm/s is achievable via a kinetic impactor and Fig. 14a indicates that a 1 mm/s impulse applied to Apophis after a 2021 timeframe launch followed by interception at Apophis's perihelion passage 7.7 years before the 2029 close approach will deflect the asteroid by 1000 km. Again, if it is desired to merely nudge Apophis away from the 2036 keyhole plus a safety margin, then a kinetic impactor of relatively low mass may suffice.

We do not compute the mass of the kinetic impactor or the parameters of the intercept trajectory herein, but the results from the section above for Apophis rendezvous provide some preliminary sizing information in terms of how much mass we can intercept Apophis with. For instance, the Heavy Lift configuration can deliver approximately 7300 kg to Apophis if no terminal rendezvous maneuver is performed.

VI. Conclusion

A spacecraft mission design architecture for designing effective NEO deflection missions has been devised, based on the authors' interpretation of the generalized hazardous NEO scenario. This architecture is recommended for use in the design of a hazardous NEO deflection mission should the need to deploy such a mission ever arise.

Approximate launch windows for efficient rendezvous with Apophis between the current time and the 2036 timeframe have been identified and the amount of mass that can be delivered to Apophis during each launch window has been characterized for both heavy lift and Discovery class mission profiles. In particular there are two excellent opportunities to rendezvous with Apophis between now and the 2029 close approach; the first around 2012 and the second around 2021. We recommend sending a scientific characterization mission to Apophis in the 2012 timeframe to determine whether a 2021 deflection mission is required in order to avert 2029 keyhole passage and to acquire the detailed physical data on Apophis required to design an effective deflection system if one is required. The physical data gathered by a mission to Apophis in 2012 will be scientifically valuable in any case.

Generalized algorithms for optimizing the deflection of a NEO via a single applied impulse were presented in detail and then applied to the Apophis scenario, showing by how much Apophis can be deflected for various impulsive velocity change magnitudes and various times of deflection between now and shortly before the 2029 close approach. This case study fully specifies the optimized deflection profile for Apophis in specific and highlights

trends in the deflection solution space in general. These algorithms are trivially parallelizable and thus well-suited to operating on a high performance computing cluster.

Regarding the use of a nuclear device to impart an impulse to a NEO, algorithms must be devised that account for NEO shape and topology to determine where to detonate the nuclear explosive in space near the NEO in order for the vaporized NEO surface material jet to generate an impulse that is oriented as desired for maximum effect. On-orbit testing will be required to validate and refine these models. Towards this end, the authors recommend the design and deployment of a campaign of test missions to harmless NEOs for the purposes of testing the concept of applying an optimally-oriented impulse to a NEO via a nuclear detonation and refining the associated algorithms.

Acknowledgments

References

[1] Barbee, B., "Mission Planning for the Mitigation of Hazardous Near Earth Objects," Master's Thesis, The University of Texas at Austin, 2005.

[2] Holsapple, Keith A. "About deflecting asteroids and comets" *Mitigation of Hazardous Asteroids and Comets,* Cambridge University Press, 2004.

[3] Barbee, B., "Project Sentinel Iteration II: A Continuation of Asteroid Deflection by Standoff Nuclear Detonation," Graduate Design Report, The University of Texas at Austin, Department of Aerospace Engineering and Engineering Mechanics, 2004.

[4] Barbee, B., Fowler, W., Davis, G., and Gaylor, D., "Optimal Deflection of Hazardous Near-Earth Objects and Mitigation Mission Design Using Current Technology," 2006 NASA Near-Earth Object Detection and Threat Mitigation Workshop, Vail, CO, June 26-29, 2006.

[5] Barbee, B., Gertsch, L., and Fowler, W., "Spacecraft Mission Design for the Destruction of Hazardous Near-Earth Objects (NEOs) via Distributed-Energy Explosives," Planetary Defense Conference, Washington DC, 2007.

[6] Ball, A. J., *et al.* "Lander and penetrator science for near-Earth object mitigation studies" *Mitigation of Hazardous Asteroids and Comets*, Cambridge University Press, 2004.